Supplementary materials

A network medicine approach for identifying diagnostic and prognostic biomarkers and exploring drug repurposing in human cancer

Le Zhang[1,#], Shiwei Fan[1,#], Julio Vera[2,3,4], Xin Lai[2,3,4,*]

1. College of Computer Science, Sichuan University, Chengdu, China
2. Laboratory of Systems Tumor Immunology, Department of Dermatology, Universitätsklinikum Erlangen and Friedrich-Alexander-Universität Erlangen-Nürnberg, Erlangen, Germany
3. Deutsches Zentrum Immuntherapie, Erlangen, Germany
4. Comprehensive Cancer Center Erlangen, Erlangen, Germany

[#]Equal contributors

[*]To whom correspondence should be addressed. E-mail: xin.lai@uk-erlangen.de

Supplementary table captions.

Table S1 Differentially expressed genes in 18 cancer types. The file contains 18 sheets, each listing significantly differentially expressed genes with log2 fold-change (tumor vs normal samples) and adjusted p-value for one cancer type.

Table S2 Gene set enrichment analyses in 18 cancer types. The file contains 18 sheets, each listing the hallmarks-of-cancer gene sets in which differentially expressed genes are significantly enriched for one cancer type. The columns from left to right are hallmark terms, the total number of genes in the hallmark term, normalized enrichment score, p-value, adjusted p-value, and the genes enriched in the hallmark term.

Table S3 Cancer type-specific networks. The file contains 18 sheets, each providing information for reconstructing a cancer type-specific network. The columns from left to right are source genes, target genes, interaction type (1: stimulation, 0: undirected, -1: inhibition), and edge weight quantified by Pearson correlation coefficients.

Table S4 Scores of nodes in cancer networks. The file contains 18 sheets, each listing scores of nodes computed by the network method for a cancer type. The columns from left to right are gene names, node degree, log2 fold-change of gene expression (tumor vs normal samples), node score, and node rank according to node score. The genes highlighted in yellow are those showing the best performance for sample classification and thus regarded as cancer genes.

Table S5 Comparisons of performances of classifiers. The table shows the performance metrics of the classifiers trained in this study or from the literature. The pan-cancer classifiers from the literature include a regularized multi-task learning model in Hossain et al. (2021), a convolutional neural network model in Mostavi et al. (2020), and a variational autoencoder model in Withnell et al. (2021).

Table S6 Results of the Cox models. The file contains 18 sheets named after a cancer type, and each sheet contains detailed information about the Cox model using genes that are derived from the network method (network) or fold-changes in expression (log2fc). The information includes the penalty parameter (λ) that gives the minimum error, the calculated error squares

and their estimated standard deviation, and the hazard ratio values of the corresponding genes (in capital letters).

Table S7 Drug information. The file contains drug annotations used in the drug repurposing analysis. The columns from left to right are identifiers of the DrugBank database, the drugs' names, targets, and FDA-approved treated cancer types by the drugs (the abbreviated names stand for the 18 cancer types investigated in this study).

Table S8 Networks for drug repurposing analysis. The file contains 14 sheets named after a cancer type plus a suffix '_node' or '_edge'. The node sheets provide information on the relevant genes, including gene names, log2 fold-change of gene expression (tumor vs normal samples), adjusted p-value for expression change, and gene category (drug targets, cancer genes, first neighbor of drug targets, and other genes on the shortest path between drug targets and cancer genes). The edge sheets provide the interactions and their weights quantified by Pearson correlation coefficients. Drug-gene interactions do not have weights.

Supplementary figure captions

The supplementary figures are presented after the figure captions.

Figure S1 Flowchart of the computational methods used for conducting the analysis. The network medicine approach contains several modules (grey blocks). In each module, we showed the data (yellow rectangles), method and model used for analysis (purple rectangles), intermediate data (green rectangles), and final results (blue rectangles). The communication between different parts of a module is connected using thin arrowed lines. Cross communication between modules is connected using thin and thick arrowed lines. The texts in the parentheses are the corresponding source of the data, the packages and methods used by us, tables (Tab.), or figures (Fig.) presented in the article. DGE: differential gene expression. GSEA: gene set enrichment analysis.

Figure S2 Differential gene expression analysis. The heat map shows the hierarchical clustering of tumor samples (turquoise) and normal tissues (yellow) using significantly differentially expressed genes ($|\log2 \text{ fold-change}| \geq 2$ and adjusted p-value ≤ 0.05). We performed the hierarchical clustering using Euclidean distance with the average linkage algorithm.

Figure S3 Principal component analysis. The plot shows the clustering of tumor samples (blue) and normal tissues (yellow) in a reduced dimensional space. We performed the analysis using significantly differentially expressed genes.

Figure S4 Cancer networks. The plot shows the largest connected component for each of the 18 cancer-specific networks. The size of nodes is proportional to their node degree (in-degree plus out-degree). The node color visualizes log fold-changes of gene expression (tumor vs normal samples). The edge color visualizes the Pearson correlation between genes.

Figure S5 Node degree distribution of cancer networks. The plot shows the distribution of the node degree in cancer-specific networks. The line is fitted to the points using a linear function. The degree follows a power-law distribution in all 18 networks, i.e. few genes have many interactions and most genes have few interactions. The information that specifies FDA-

approved drugs for specific cancers was gathered from the NCI website (www.cancer.gov/about-cancer/treatment/drugs/cancer-type).

Figure S6 Hierarchical clustering of tumor and normal samples. The heat map shows the hierarchical clustering of tumor samples (turquoise) and normal tissues (yellow) using network-derived genes (**A**) or aberrantly expressed genes (**B**). We performed the hierarchical clustering using Euclidean distance with the average linkage algorithm. The genes were selected by the random forests that showed the best metrics in sample classification (Table 2).

Figure S7 Network topology analysis. The bar plot shows the ranking of four centrality values (such as degree, closeness, betweenness, and eigenvalue centrality) of the identified cancer genes in the networks. Degree centrality indicates how many connections each gene has to other genes in the network. Closeness centrality calculates the shortest paths between all genes, then assigns each gene a score based on its sum of shortest paths. Betweenness centrality shows which genes are 'bridges' between genes in a network. It does this by identifying all the shortest paths and then counting how many times each gene falls on one. Eigenvalue centrality shows that the centrality of a gene is proportional to the sum of the centralities of its direct neighbor genes. The y-axis is the percentile ranking of a gene using different centrality values (the higher the better ranking of a gene in the network), and the x-axis is the name of the cancer genes.

Figure S8 Density plots of p-values from the survival analyses using single genes. We used 10 (**A**), 20 (**B**), 50 (**C**) and 100 (**D**) genes to compare the performance of genes ranked by the network method (network) or fold-changes in expression (log2fc) in survival analyses. For each gene, we divided patients into high-expression (top 50%) and low-expression (remaining 50%) groups and performed Kaplan-Meier analysis (two-sided log-rank test). The p-values of the estimates were used to draw the density plots. To determine whether there were any differences in the distribution of p-values, we performed the Fisher-Pitman permutation test and added its calculated p-value at the top of the plots. The numbers in parentheses give the number of joint genes between the two ranking methods.

Figure S9 Comparison of survival analyses using combined genes. We used the combined genes identified by the network method (**A**) or fold-changes in expression (**B**) to compare their abilities in predicting cancer patients' survival rates. The patients were divided into high-risk and

low-risk groups using the scores computed by a Cox regression model. The p-value of the survival curves was obtained using a two-sided log-rank test.

Figure S10 Drug distance to cancer gene and normal gene sets. The bar plot shows the distance of the identified repurposable drugs (x-axis) to cancer or normal genes in cancer networks. For each cancer type, its cancer gene set was identified using the network method while the counterpart is a normal gene set with high average expression in normal tissues and many interacting genes. The normal gene set contains top *n* genes (*n* equals to the number of genes in the corresponding cancer get set). The genes were ranked by a score that multiplies the average expression of a gene in normal tissues with the gene's node degree in the network. The y-axis indicates the distance from the drug targets to the genes in both gene sets (see Materials and Methods).

Figure S11 Shortest paths between the repurposed drugs and cancer genes in KIRP (A) and LUAD (B). The paths were derived from the corresponding cancer-specific networks. Drugs and genes are shown as diamonds and circles, respectively. The node colors indicate the direction of gene expression change (red: upregulation; blue: downregulation). The label colors represent different gene categories: drug target genes (purple), cancer genes (orange), and other genes (grey) on the shortest path between drug targets and cancer genes. The edge colors visualizes the interaction type between genes (pink: stimulation; green: inhibition); drug-target interactions are shown in black. The data illustrated in the network can be found in Table S8. DB06616: bosutinib; DB08865: crizotinib; DB01254: dasatinib; DB00317: gefitinib; DB04868: nilotinib; DB05294: vandetanib.

Figure S12 Cancer cell lines' sensitivity to the identified repurposable drugs. The plot shows the ranking (x-axis) of the drugs based on their measured IC50 values (y-axis) in corresponding cancer cell lines (dots) for specific drugs. The higher ranking (more left on the x-axis) of a cell line the more sensitive it is to a specified drug. The IC50 values of cell lines fall between the dashed black lines (i.e., maximum and minimum drug screening concentrations) indicating that the cell lines are sensitive (highlighted in green) to the drug otherwise resistant (highlighted in red). The figures were downloaded from the GDSC database and adapted.

Figure S1

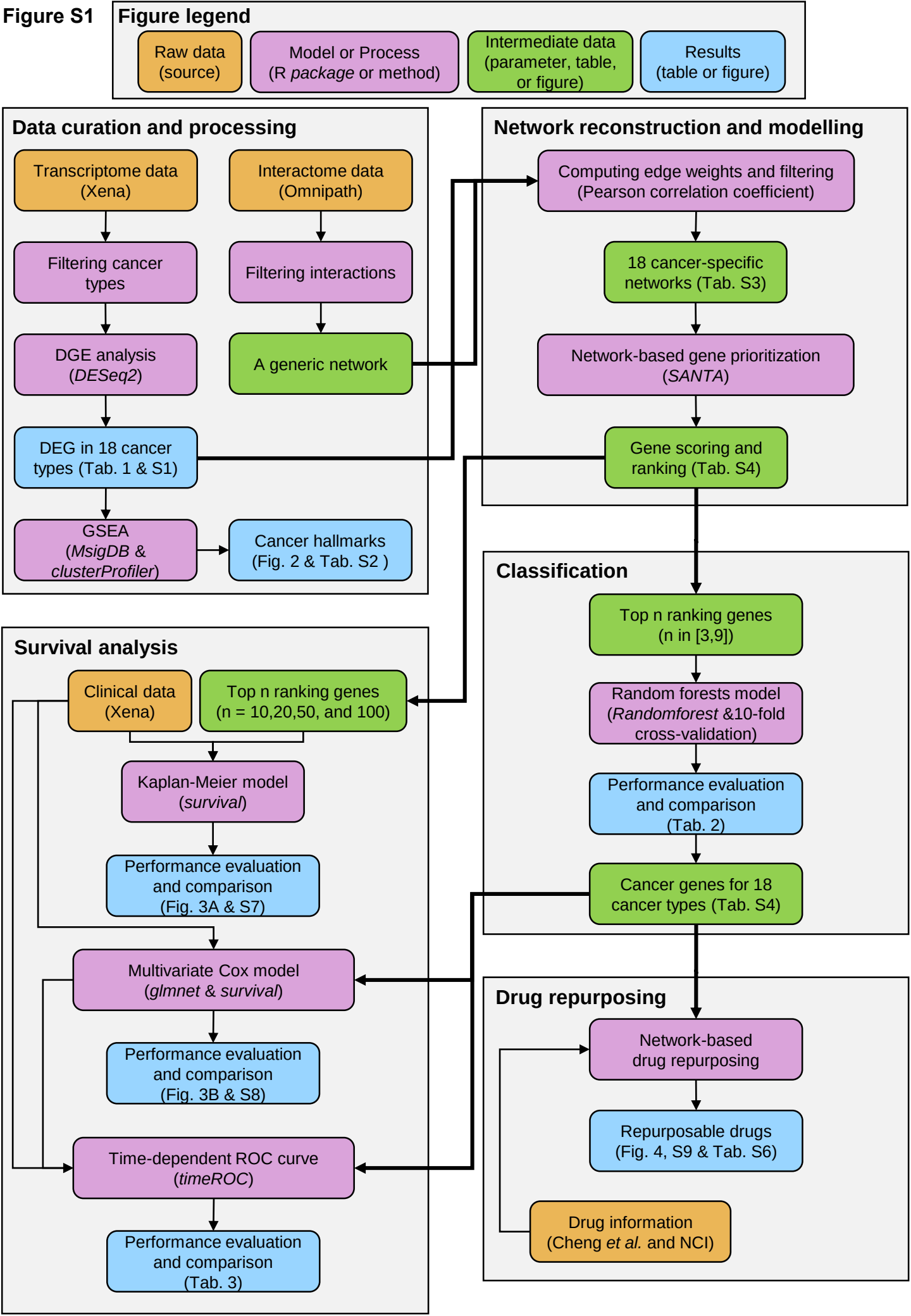
Figure legend
Raw data (source)
Model or Process (R package or method)
Intermediate data (parameter, table, or figure)
Results (table or figure)
Data curation and processing
Transcriptome data (Xena)
Interactome data (Omnipath)
Filtering cancer types
Filtering interactions
DGE analysis (DESeq2)
A generic network
DEG in 18 cancer types (Tab. 1 & S1)
GSEA (MsigDB & clusterProfiler)
Cancer hallmarks (Fig. 2 & Tab. S2)
Network reconstruction and modelling
Computing edge weights and filtering (Pearson correlation coefficient)
18 cancer-specific networks (Tab. S3)
Network-based gene prioritization (SANTA)
Gene scoring and ranking (Tab. S4)
Classification
Top n ranking genes (n in [3,9])
Random forests model (Randomforest &10-fold cross-validation)
Performance evaluation and comparison (Tab. 2)
Cancer genes for 18 cancer types (Tab. S4)
Survival analysis
Clinical data (Xena)
Top n ranking genes (n = 10,20,50, and 100)
Kaplan-Meier model (survival)
Performance evaluation and comparison (Fig. 3A & S7)
Multivariate Cox model (glmnet & survival)
Performance evaluation and comparison (Fig. 3B & S8)
Time-dependent ROC curve (timeROC)
Performance evaluation and comparison (Tab. 3)
Drug repurposing
Network-based drug repurposing
Repurposable drugs (Fig. 4, S9 & Tab. S6)
Drug information (Cheng et al. and NCI)

Figure S2

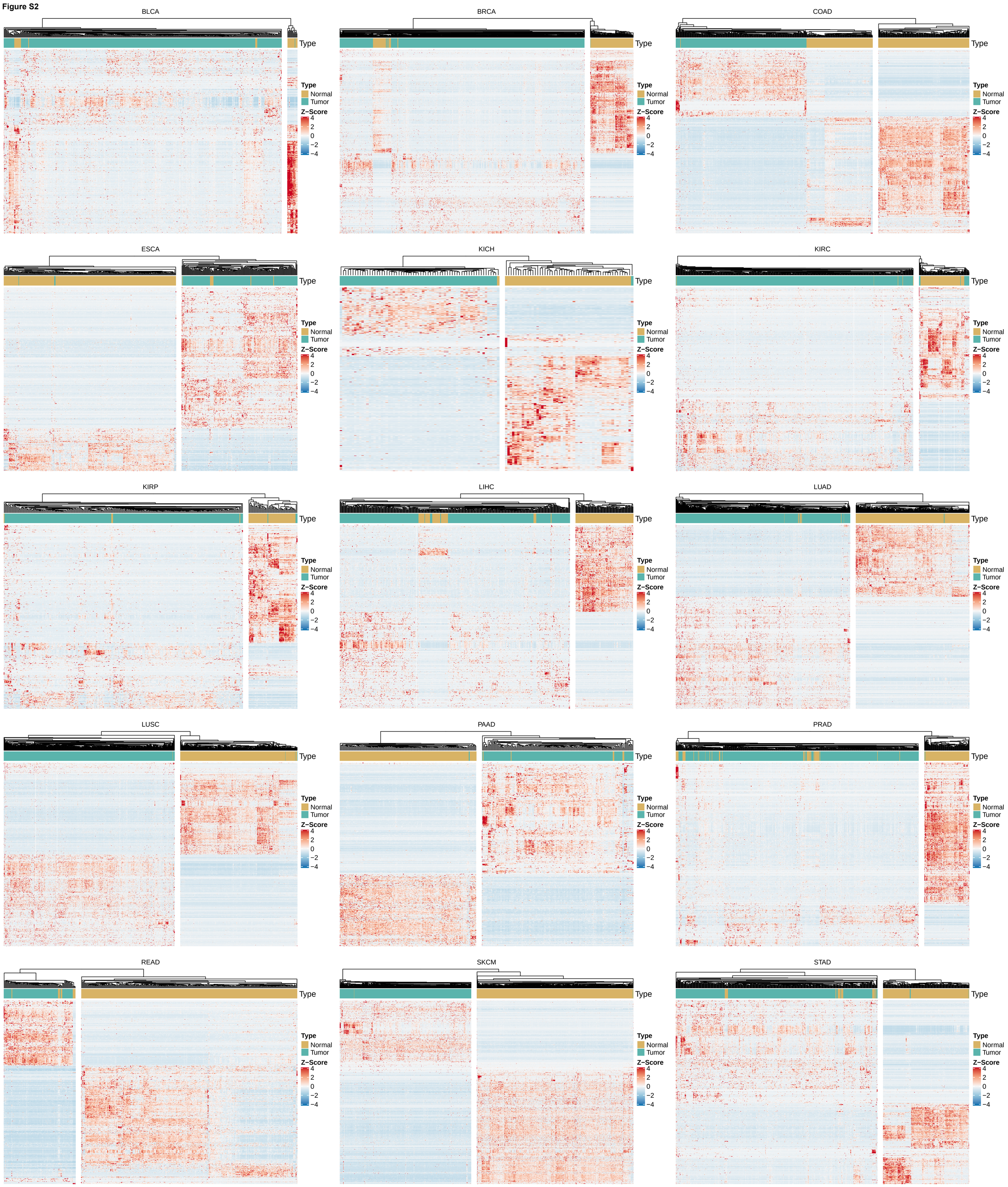
BLCA
BRCA
COAD
ESCA
KICH
KIRC
KIRP
LIHC
LUAD
LUSC
PAAD
PRAD
READ
SKCM
STAD
THCA
THYM
UCEC
Type
Type
Normal
Tumor
Z−Score
4
2
0
−2
−4

Figure S3

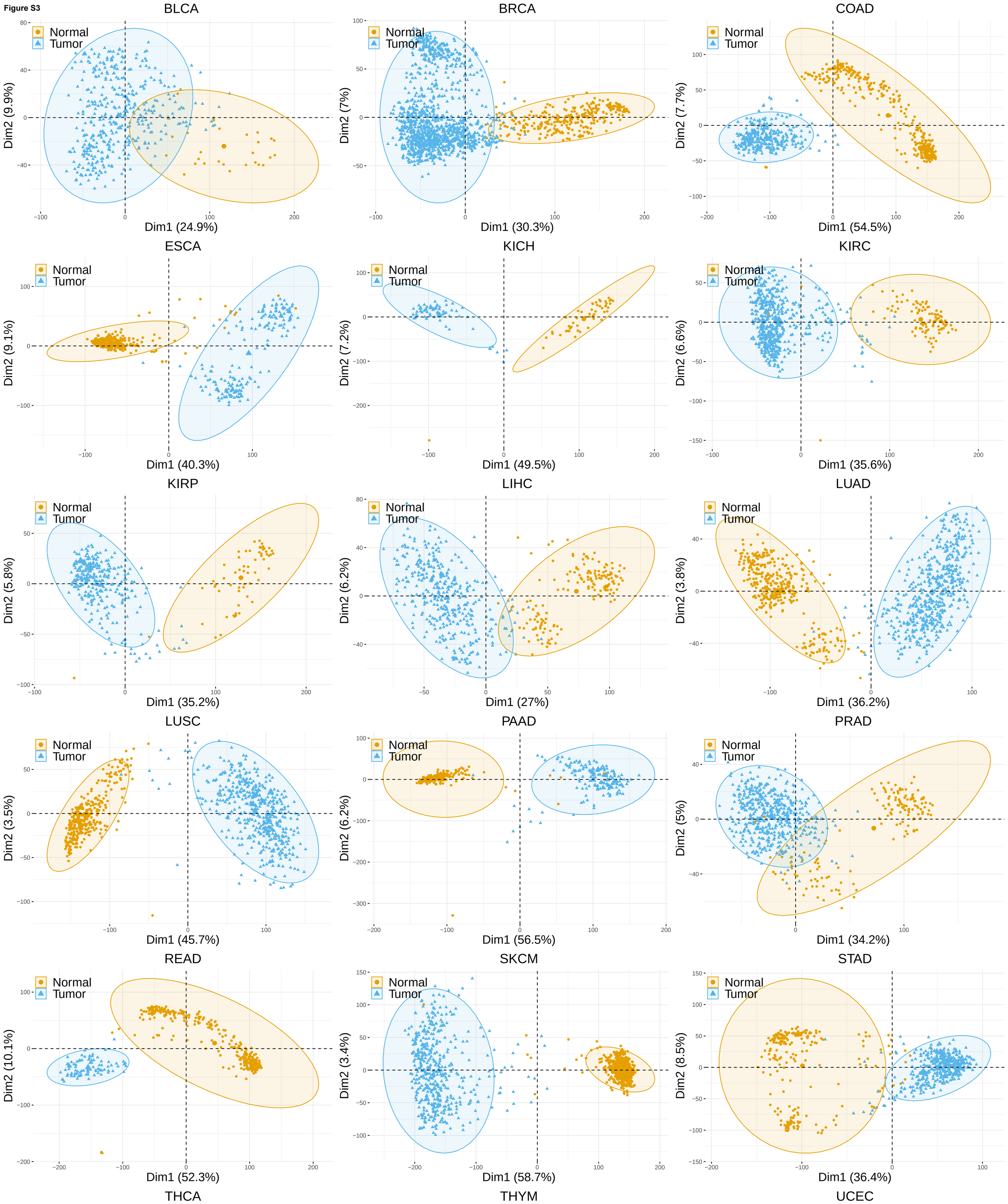
BLCA
Normal
Tumor
Dim2 (9.9%)
Dim1 (24.9%)
BRCA
Dim2 (7%)
Dim1 (30.3%)
COAD
Dim2 (7.7%)
Dim1 (54.5%)
ESCA
Dim2 (9.1%)
Dim1 (40.3%)
KICH
Dim2 (7.2%)
Dim1 (49.5%)
KIRC
Dim2 (6.6%)
Dim1 (35.6%)
KIRP
Dim2 (5.8%)
Dim1 (35.2%)
LIHC
Dim2 (6.2%)
Dim1 (27%)
LUAD
Dim2 (3.8%)
Dim1 (36.2%)
LUSC
Dim2 (3.5%)
Dim1 (45.7%)
PAAD
Dim2 (6.2%)
Dim1 (56.5%)
PRAD
Dim2 (5%)
Dim1 (34.2%)
READ
Dim2 (10.1%)
Dim1 (52.3%)
SKCM
Dim2 (3.4%)
Dim1 (58.7%)
STAD
Dim2 (8.5%)
Dim1 (36.4%)
THCA
Dim2 (8.1%)
Dim1 (45.9%)
THYM
Dim2 (5.9%)
Dim1 (57.1%)
UCEC
Dim2 (4.5%)
Dim1 (46.7%)

Figure S4

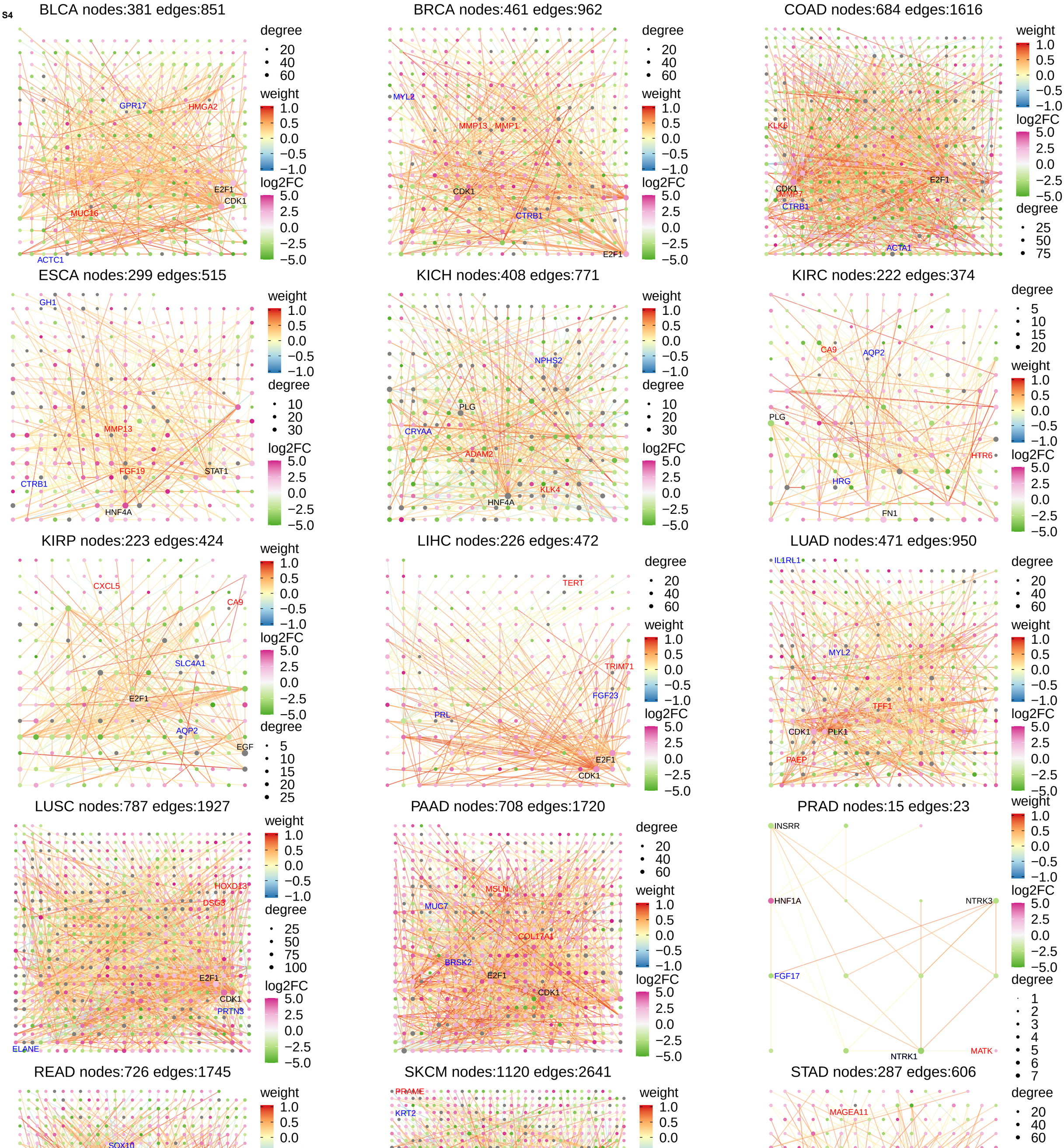
BLCA nodes:381 edges:851
GPR17
HMGA2
E2F1
CDK1
MUC16
ACTC1
BRCA nodes:461 edges:962
MYL2
MMP13
MMP1
CDK1
CTRB1
E2F1
COAD nodes:684 edges:1616
KLK6
E2F1
CDK1
MMP7
CTRB1
ACTA1
ESCA nodes:299 edges:515
GH1
MMP13
FGF19
STAT1
CTRB1
HNF4A
KICH nodes:408 edges:771
NPHS2
PLG
CRYAA
ADAM2
KLK4
HNF4A
KIRC nodes:222 edges:374
CA9
AQP2
PLG
HTR6
HRG
FN1
KIRP nodes:223 edges:424
CXCL5
CA9
SLC4A1
E2F1
AQP2
EGF
LIHC nodes:226 edges:472
TERT
TRIM71
FGF23
PRL
E2F1
CDK1
LUAD nodes:471 edges:950
IL1RL1
MYL2
TFF1
CDK1
PLK1
PAEP
LUSC nodes:787 edges:1927
HOXD13
DSG3
E2F1
CDK1
PRTN3
ELANE
PAAD nodes:708 edges:1720
MSLN
MUC7
COL17A1
BRSK2
E2F1
CDK1
PRAD nodes:15 edges:23
INSRR
HNF1A
NTRK3
FGF17
NTRK1
MATK
READ nodes:726 edges:1745
SOX10
GH1
FGF19
E2F1
CDK1
MMP7
SKCM nodes:1120 edges:2641
PRAME
KRT2
KRTAP4-12
IGHG1
EGFR
CDK1
STAD nodes:287 edges:606
MAGEA11
FGF19
MYBPC3
CDK1
PLK1
CCKBR
THCA nodes:166 edges:300
TMPRSS6
MMP13
E2F1
DEFA1B
DEFA3
FN1
THYM nodes:2139 edges:7658
ALAS2
CTSV
HLA-B
TDGF1
HBB
EGFR
UCEC nodes:1022 edges:2582
ZIC2
PTGER3
E2F1
CDK1
AOC1
ZBTB16
degree
weight
log2FC

Figure S5

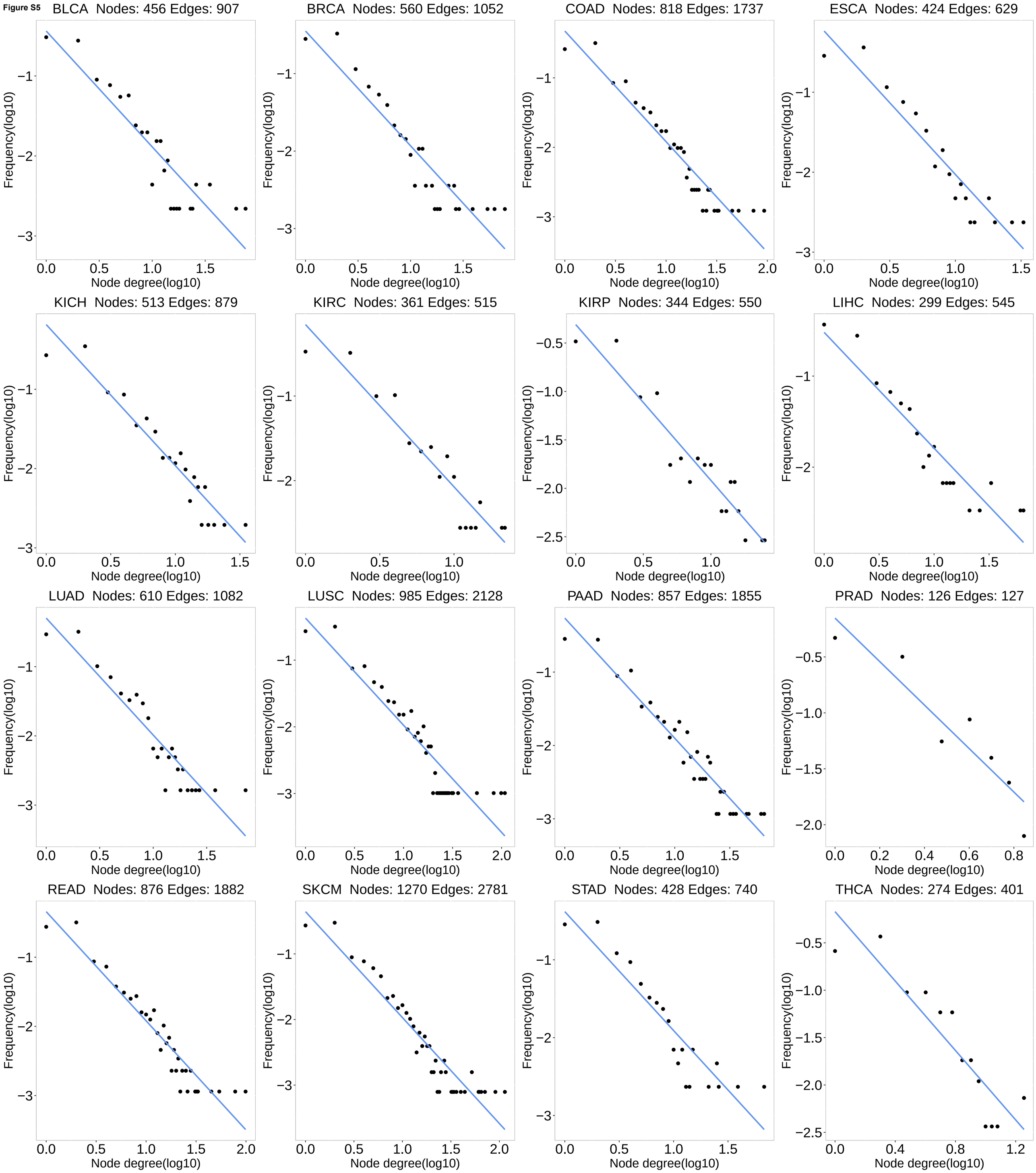
BLCA Nodes: 456 Edges: 907
BRCA Nodes: 560 Edges: 1052
COAD Nodes: 818 Edges: 1737
ESCA Nodes: 424 Edges: 629
KICH Nodes: 513 Edges: 879
KIRC Nodes: 361 Edges: 515
KIRP Nodes: 344 Edges: 550
LIHC Nodes: 299 Edges: 545
LUAD Nodes: 610 Edges: 1082
LUSC Nodes: 985 Edges: 2128
PAAD Nodes: 857 Edges: 1855
PRAD Nodes: 126 Edges: 127
READ Nodes: 876 Edges: 1882
SKCM Nodes: 1270 Edges: 2781
STAD Nodes: 428 Edges: 740
THCA Nodes: 274 Edges: 401
THYM Nodes: 2294 Edges: 7830
UCEC Nodes: 1153 Edges: 2707
Frequency(log10)
Node degree(log10)

Figure S6A

BLCA

BLCA

Type

BRCA2

PTGS2

BIN1

Type
Normal
Tumor
Z−Score
4
2
0
−2
−4

F

BRCA

Type

CCL7

MCM10

CDC25C

KIF23

KPNA2

CDT1

AKAP12

ANGPT4

FGF8

Type
Normal
Tumor
Z−Score
4
2
0
−2
−4

COAD

Type

SST

NTRK1

CAV1

PHKG1

PTPRO

MET

Type
Normal
Tumor
Z−Score
4
2
0
−2
−4

ESCA

Type

SERPINA1

AGT

MMP8

PTPRO

MET

ITGB4

SERPINE1

MMP13

Type
Normal
Tumor
Z−Score
4
2
0
−2
−4

KICH

Type

PTGIR

SLPI

SCNN1B

DAO

PROC

PON1

GRIN1

KCNH2

Type
Normal
Tumor
Z−Score
4
2
0
−2
−4

KIRC

Type

PAPPA

PDGFRA

HLA−DPA1

HLA−DPB1

CD8A

CD3G

TRBV7−9

FGA

HRG

Type
Normal
Tumor
Z−Score
4
2
0
−2
−4

KIRP

Type

WNT5A

EREG

TRPC3

PDGFRB

SLC9A3R2

NPHS1

CNTN1

SLC8A1

NOS1

Type
Normal
Tumor
Z−Score
4
2
0
−2
−4

LIHC

Type

RAD51

MCM10

MAD2L1

KIF23

CDCA8

CDKN3

BLM

UHRF1

KRT1

Type
Normal
Tumor
Z−Score
4
2
0
−2
−4

LUAD

Type

FGF5

CDH1

MET

CDC45

ORC1

PTPRB

Type
Normal
Tumor
Z−Score
4
2
0
−2
−4

LUSC

Type

EPHA8

EPHA1

EPHB3

ITGB4

KIF23

ALOX12

EPHA7

HIST1H3J

EPHA6

Type
Normal
Tumor
Z−Score
4
2
0
−2
−4

PAAD

Type

EPHA7

ROS1

MST1R

MET

AXL

Type
Normal
Tumor
Z−Score
4
2
0
−2
−4

PRAD

Type

COMP

COL2A1

NTF4

FGF17

PGF

ANGPT4

PNLIPRP2

CLPS

Type
Normal
Tumor
Z−Score
4
2
0
−2
−4

READ

Type

KPNA2

GRIN1

PHKG1

NRXN1

Type
Normal
Tumor
Z−Score
4
2
0
−2
−4

SKCM

Type

SUMO4

EPHB3

GJA1

RGN

ITGA4

FCGR1A

TYR

CDKN3

HOXB7

Type
Normal
Tumor
Z−Score
4
2
0
−2
−4

STAD

Type

MMP13

ORC6

MCM2

ORC1

CDT1

CLSPN

ECT2

TP73

Type
Normal
Tumor
Z−Score
4
2
0
−2
−4

THCA

Type

FGF23

SERPINF2

ELANE

SERPINA5

CTRB1

SERPINA1

MDK

TGFA

EREG

Type
Normal
Tumor
Z−Score
4
2
0
−2
−4

THYM

Type

HGF

RAF1

PDGFA

CHEK1

ERBB3

Type
Normal
Tumor
Z−Score
4
2
0
−2
−4

UCEC

Type

GALNT15

LRP1

GRB7

CENPF

PRC1

DTL

ITGB7

MST1R

PTPRT

Type
Normal
Tumor
Z−Score
4
2
0
−2
−4

Figure S6B

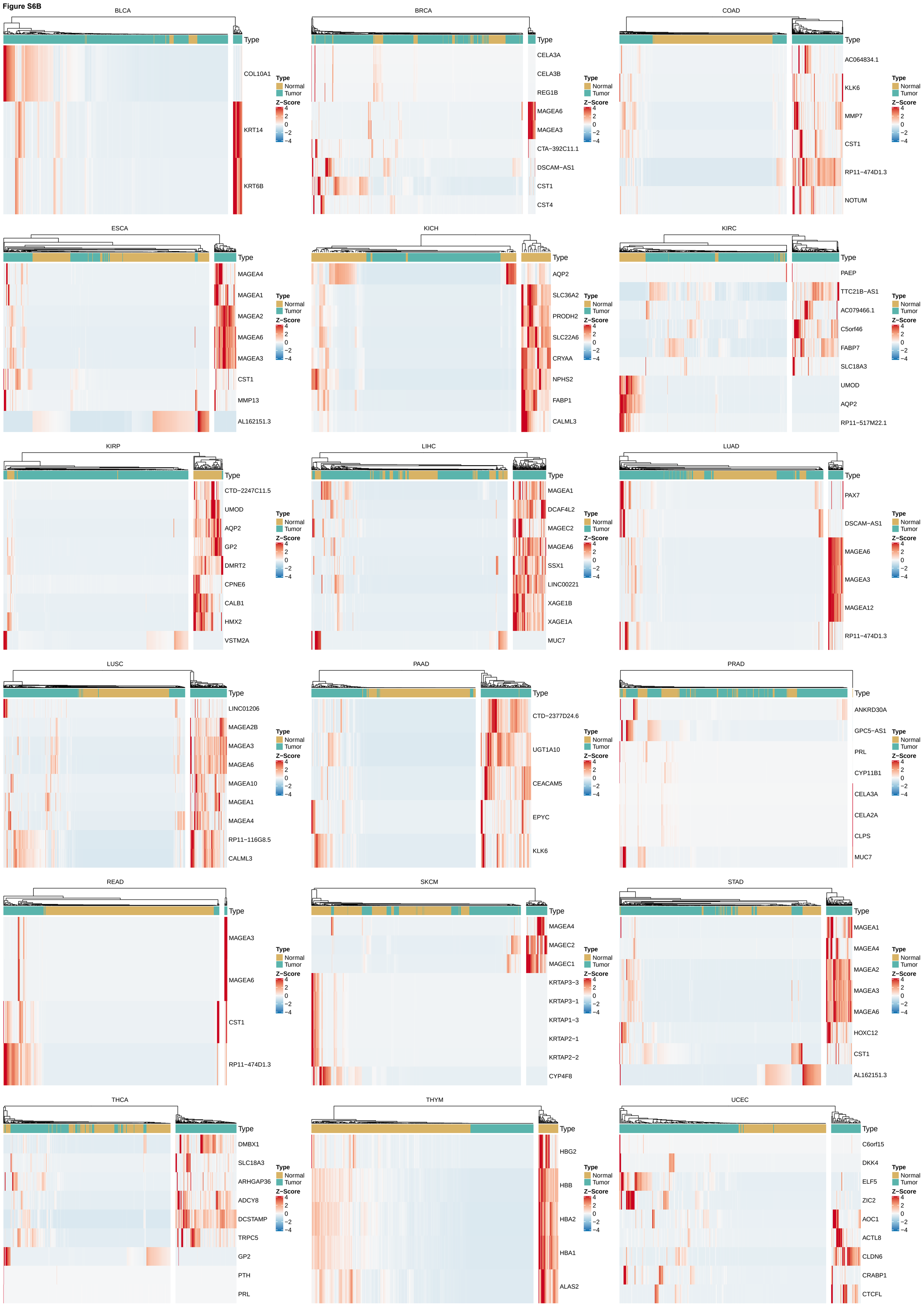
BLCA
Type
COL10A1
KRT14
KRT6B
BRCA
CELA3A
CELA3B
REG1B
MAGEA6
MAGEA3
CTA−392C11.1
DSCAM−AS1
CST1
CST4
COAD
AC064834.1
KLK6
MMP7
CST1
RP11−474D1.3
NOTUM
ESCA
MAGEA4
MAGEA1
MAGEA2
MAGEA6
MAGEA3
CST1
MMP13
AL162151.3
KICH
AQP2
SLC36A2
PRODH2
SLC22A6
CRYAA
NPHS2
FABP1
CALML3
KIRC
PAEP
TTC21B−AS1
AC079466.1
C5orf46
FABP7
SLC18A3
UMOD
AQP2
RP11−517M22.1
KIRP
CTD−2247C11.5
UMOD
AQP2
GP2
DMRT2
CPNE6
CALB1
HMX2
VSTM2A
LIHC
MAGEA1
DCAF4L2
MAGEC2
MAGEA6
SSX1
LINC00221
XAGE1B
XAGE1A
MUC7
LUAD
PAX7
DSCAM−AS1
MAGEA6
MAGEA3
MAGEA12
RP11−474D1.3
LUSC
LINC01206
MAGEA2B
MAGEA3
MAGEA6
MAGEA10
MAGEA1
MAGEA4
RP11−116G8.5
CALML3
PAAD
CTD−2377D24.6
UGT1A10
CEACAM5
EPYC
KLK6
PRAD
ANKRD30A
GPC5−AS1
PRL
CYP11B1
CELA3A
CELA2A
CLPS
MUC7
READ
MAGEA3
MAGEA6
CST1
RP11−474D1.3
SKCM
MAGEA4
MAGEC2
MAGEC1
KRTAP3−3
KRTAP3−1
KRTAP1−3
KRTAP2−1
KRTAP2−2
CYP4F8
STAD
MAGEA1
MAGEA4
MAGEA2
MAGEA3
MAGEA6
HOXC12
CST1
AL162151.3
THCA
DMBX1
SLC18A3
ARHGAP36
ADCY8
DCSTAMP
TRPC5
GP2
PTH
PRL
THYM
HBG2
HBB
HBA2
HBA1
ALAS2
UCEC
C6orf15
DKK4
ELF5
ZIC2
AOC1
ACTL8
CLDN6
CRABP1
CTCFL
Type
Normal
Tumor
Z−Score
4
2
0
−2
−4

Figure 7

BLCA

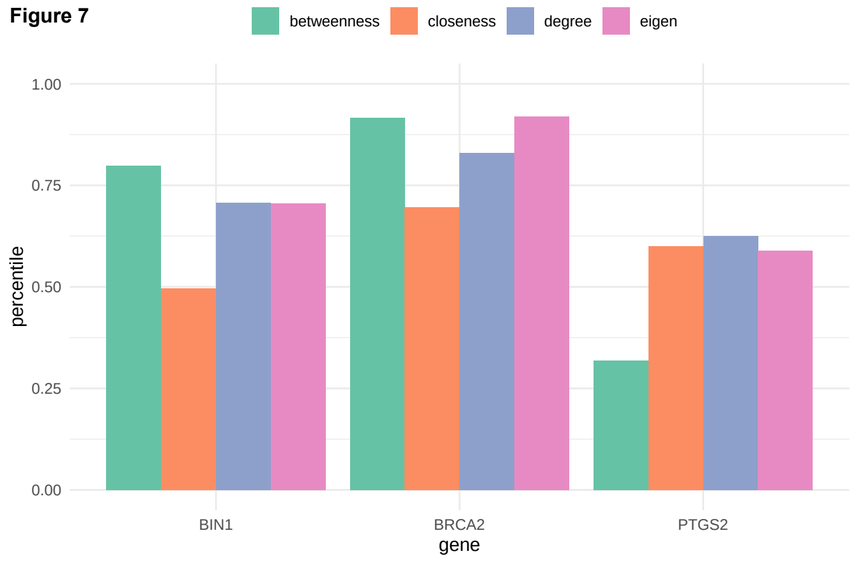

BRCA

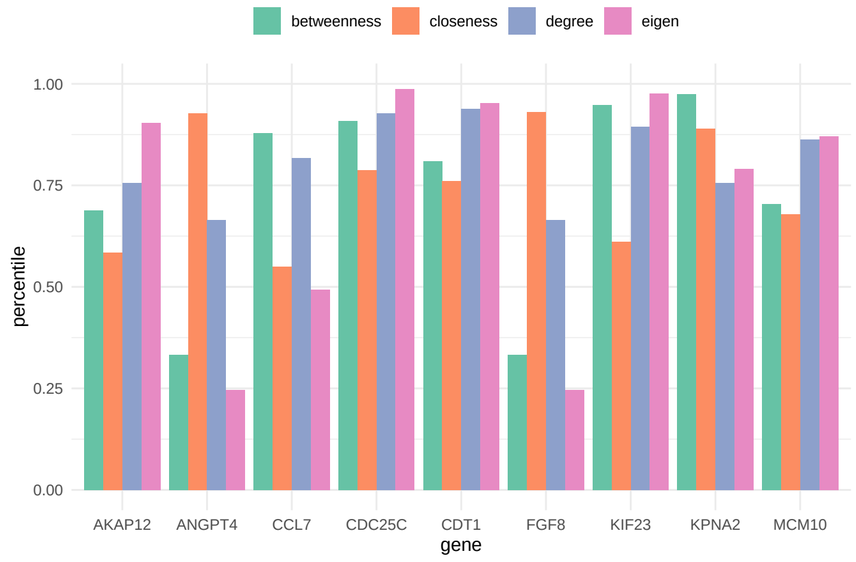

COAD

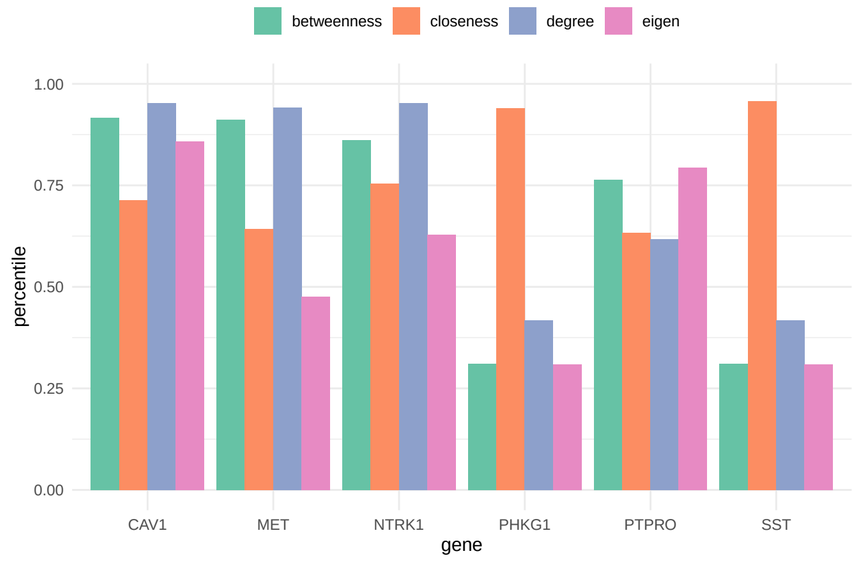

ESCA

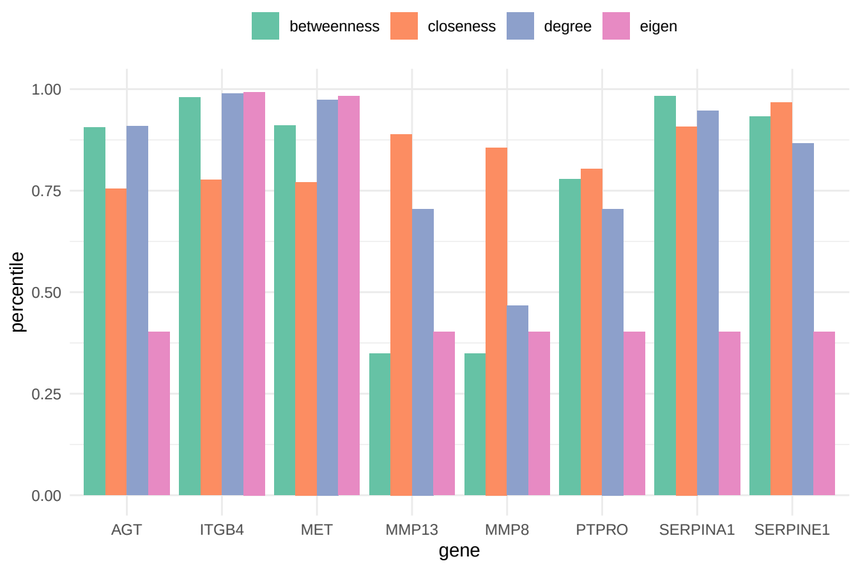

KICH

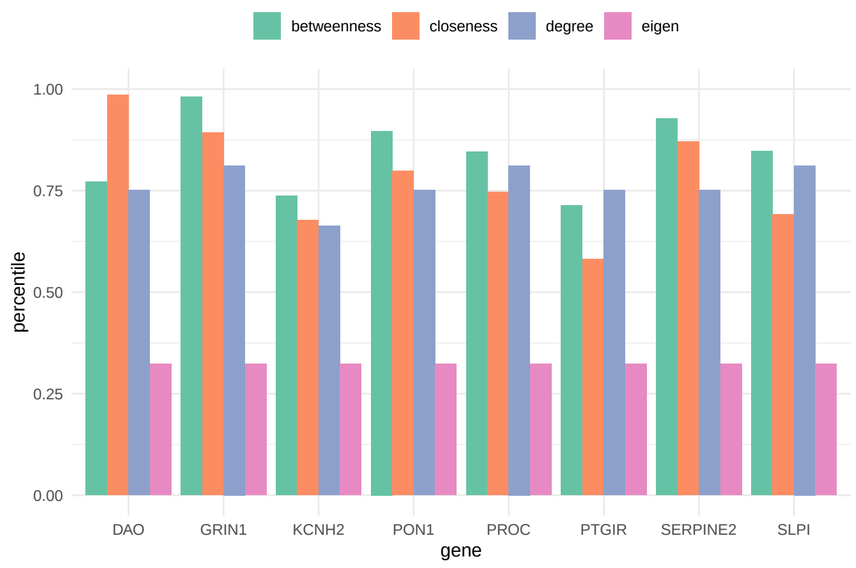

KIRC

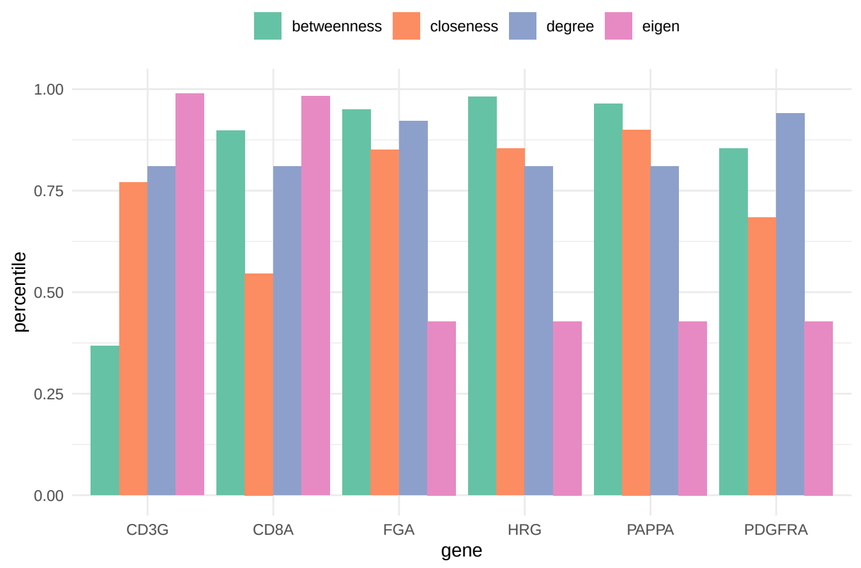

KIRP

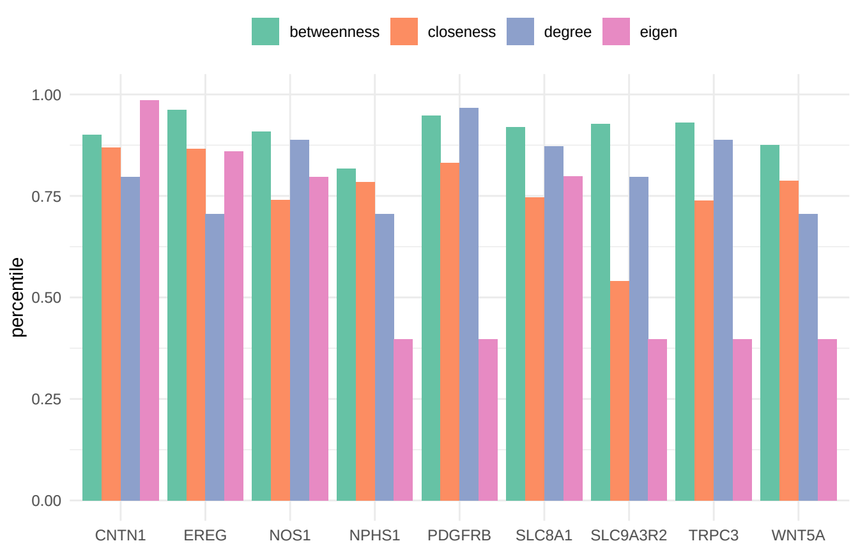

LIHC

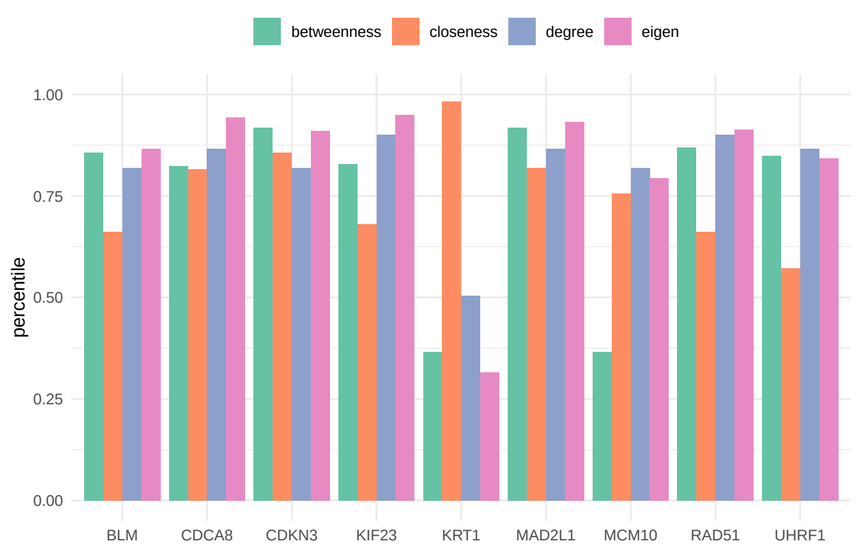

LUAD

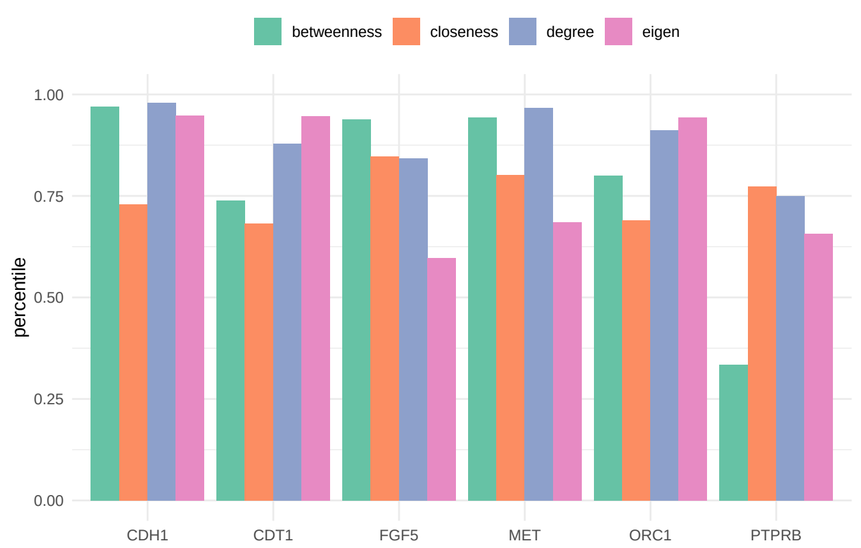

LUSC

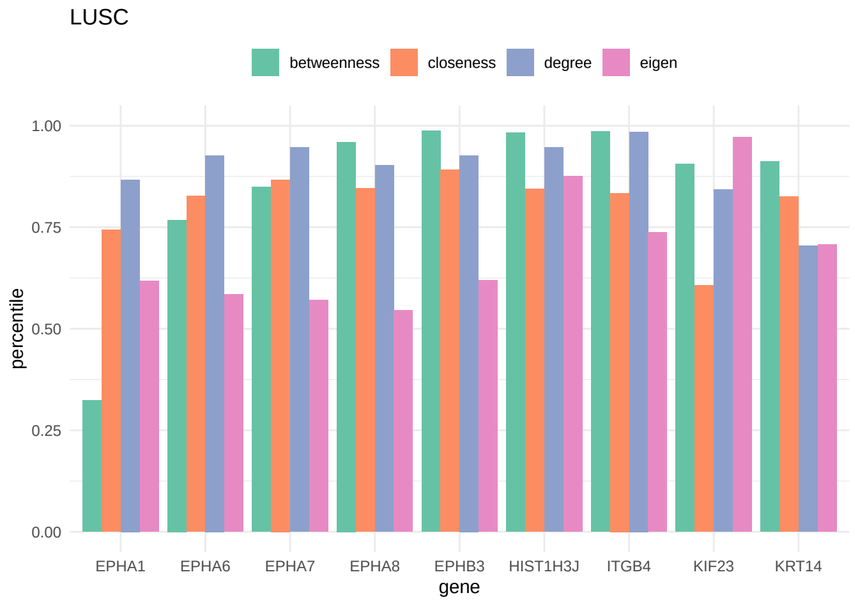

PAAD

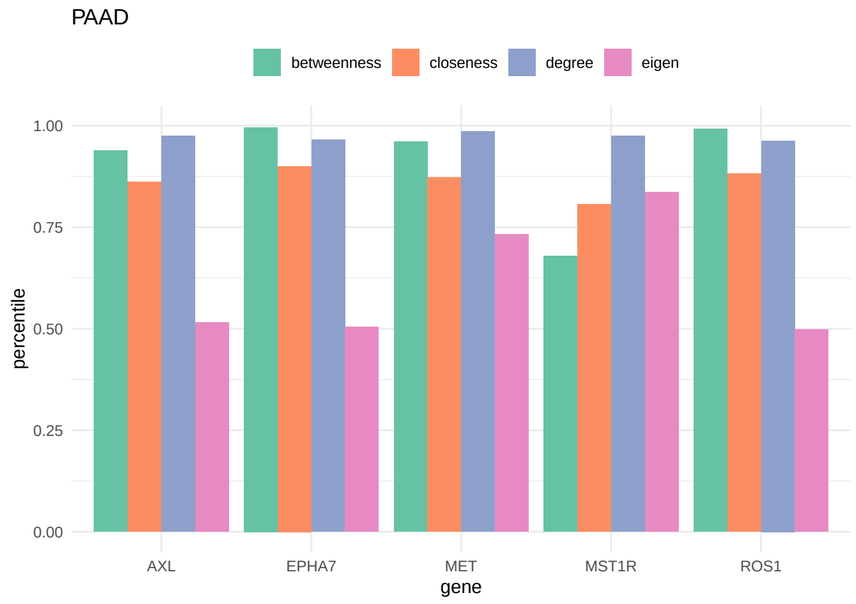

PRAD

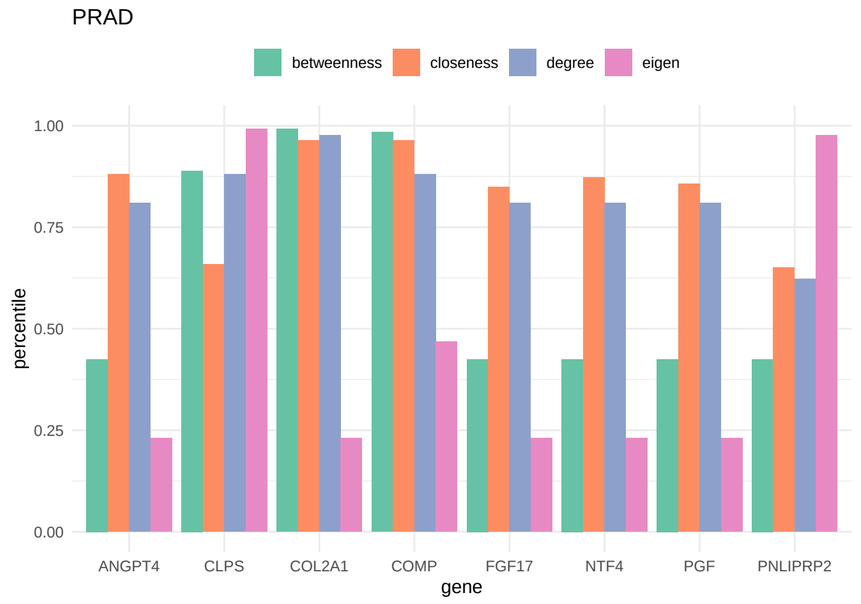

READ

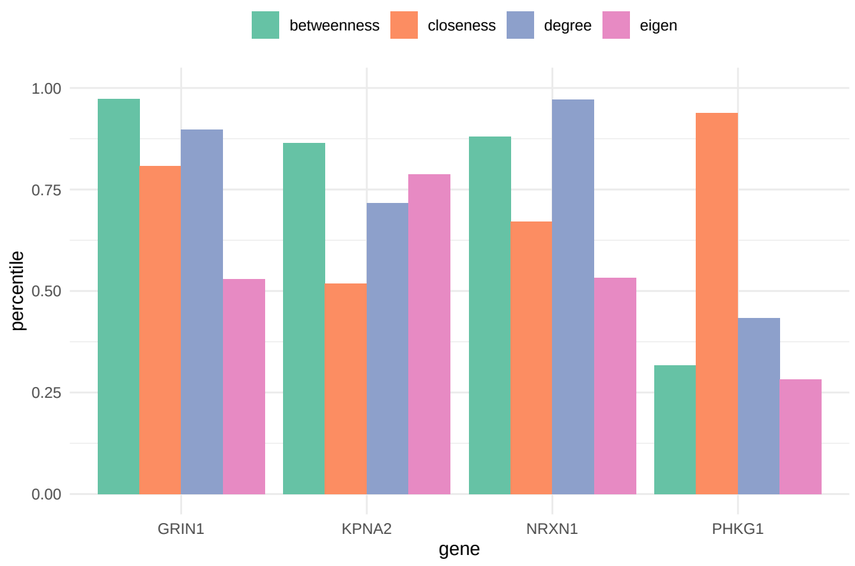

SKCM

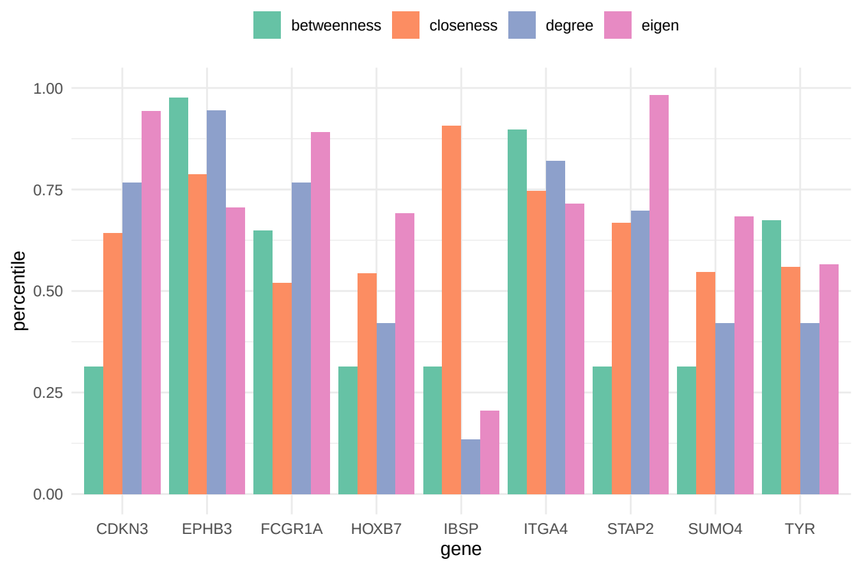

STAD

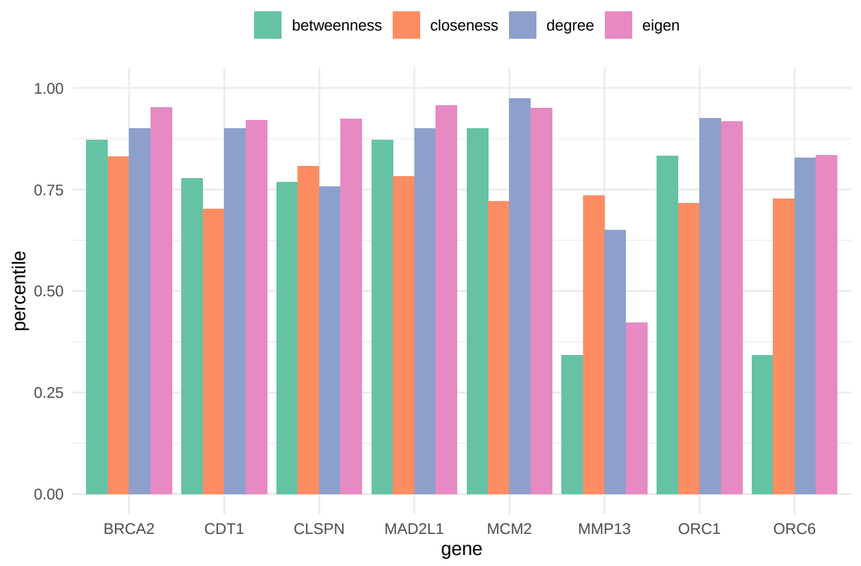

THCA

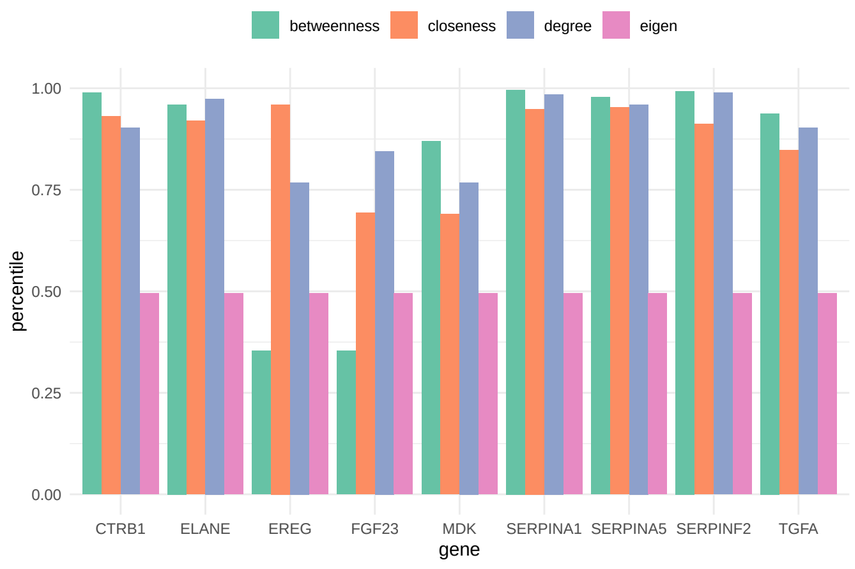

THYM

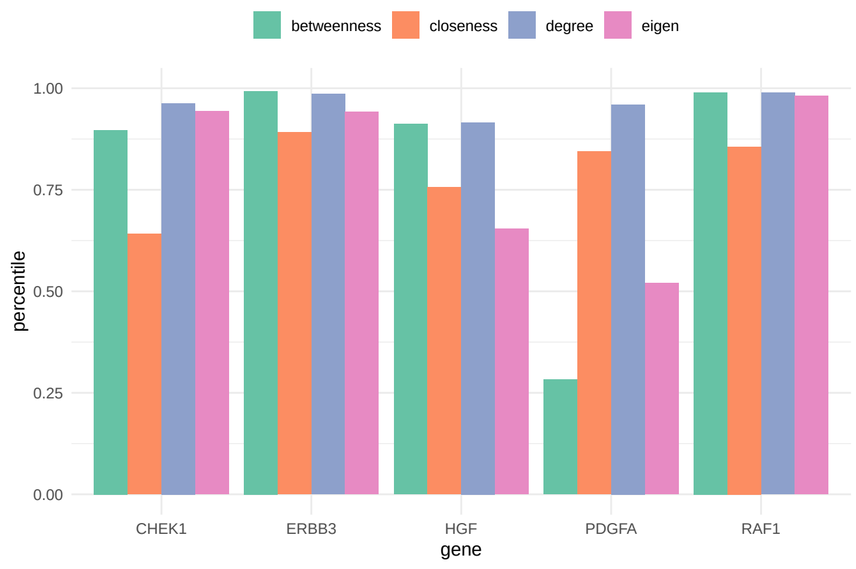

UCEC

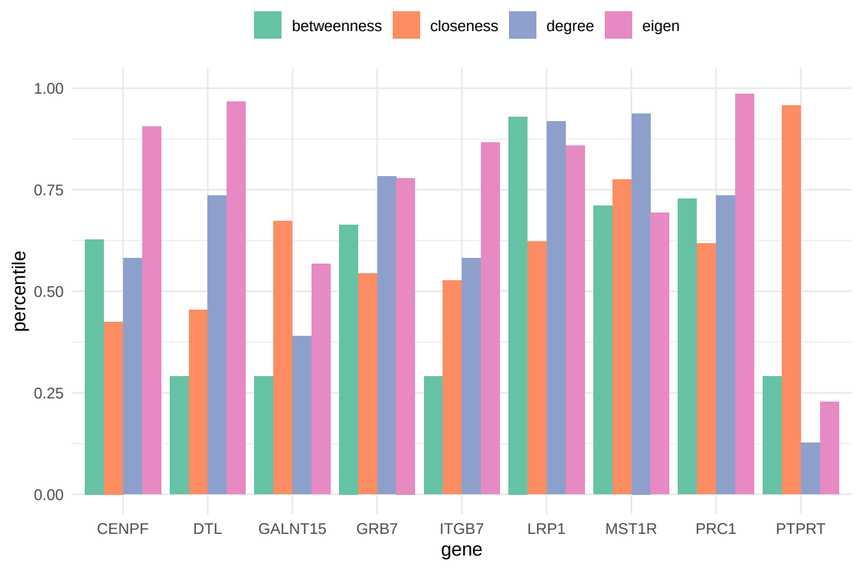

Figure S8A

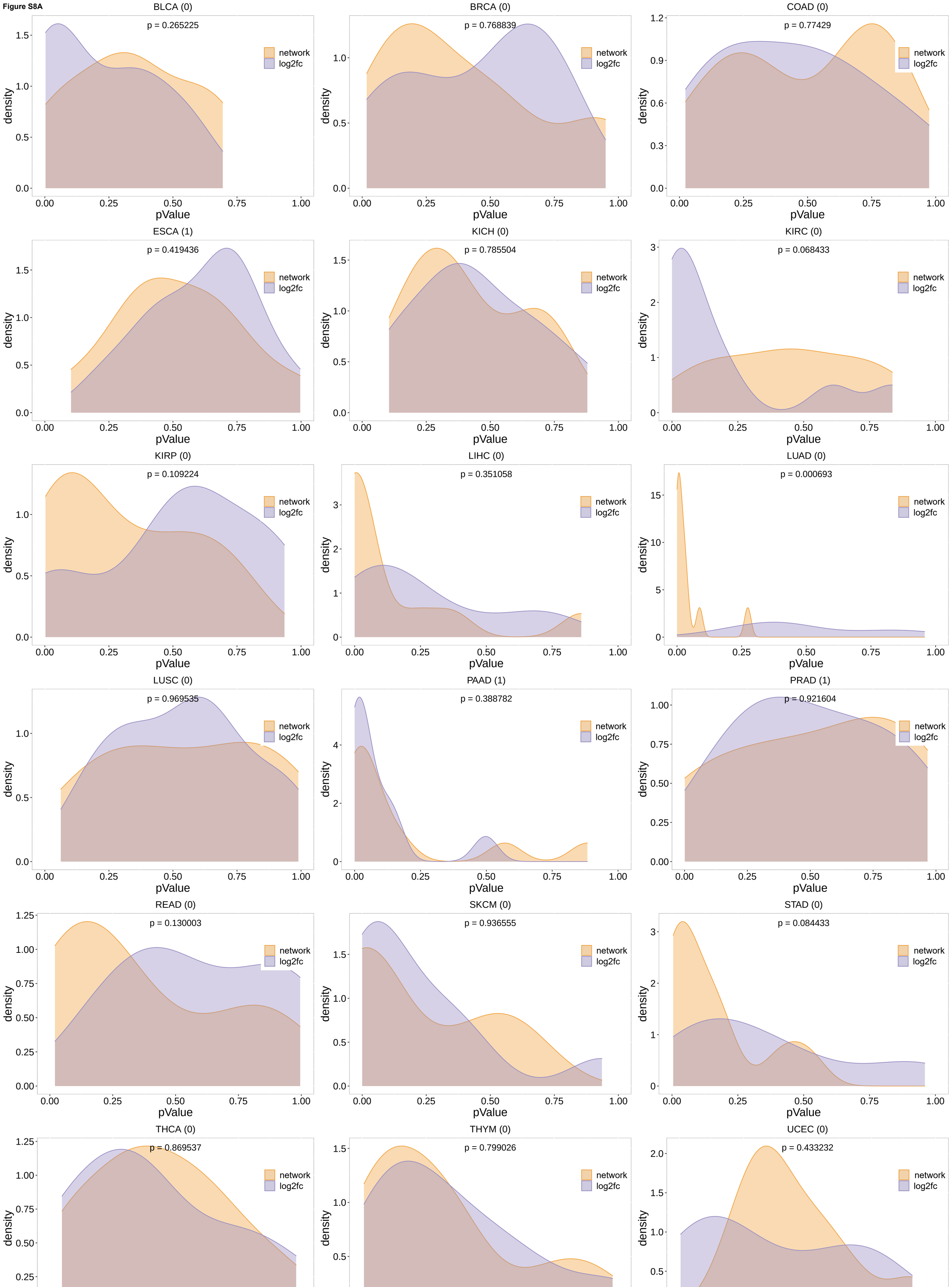
BLCA (0)
p = 0.265225
BRCA (0)
p = 0.768839
COAD (0)
p = 0.77429
ESCA (1)
p = 0.419436
KICH (0)
p = 0.785504
KIRC (0)
p = 0.068433
KIRP (0)
p = 0.109224
LIHC (0)
p = 0.351058
LUAD (0)
p = 0.000693
LUSC (0)
p = 0.969535
PAAD (1)
p = 0.388782
PRAD (1)
p = 0.921604
READ (0)
p = 0.130003
SKCM (0)
p = 0.936555
STAD (0)
p = 0.084433
THCA (0)
p = 0.869537
THYM (0)
p = 0.799026
UCEC (0)
p = 0.433232
network
log2fc
density
pValue

Figure S8B

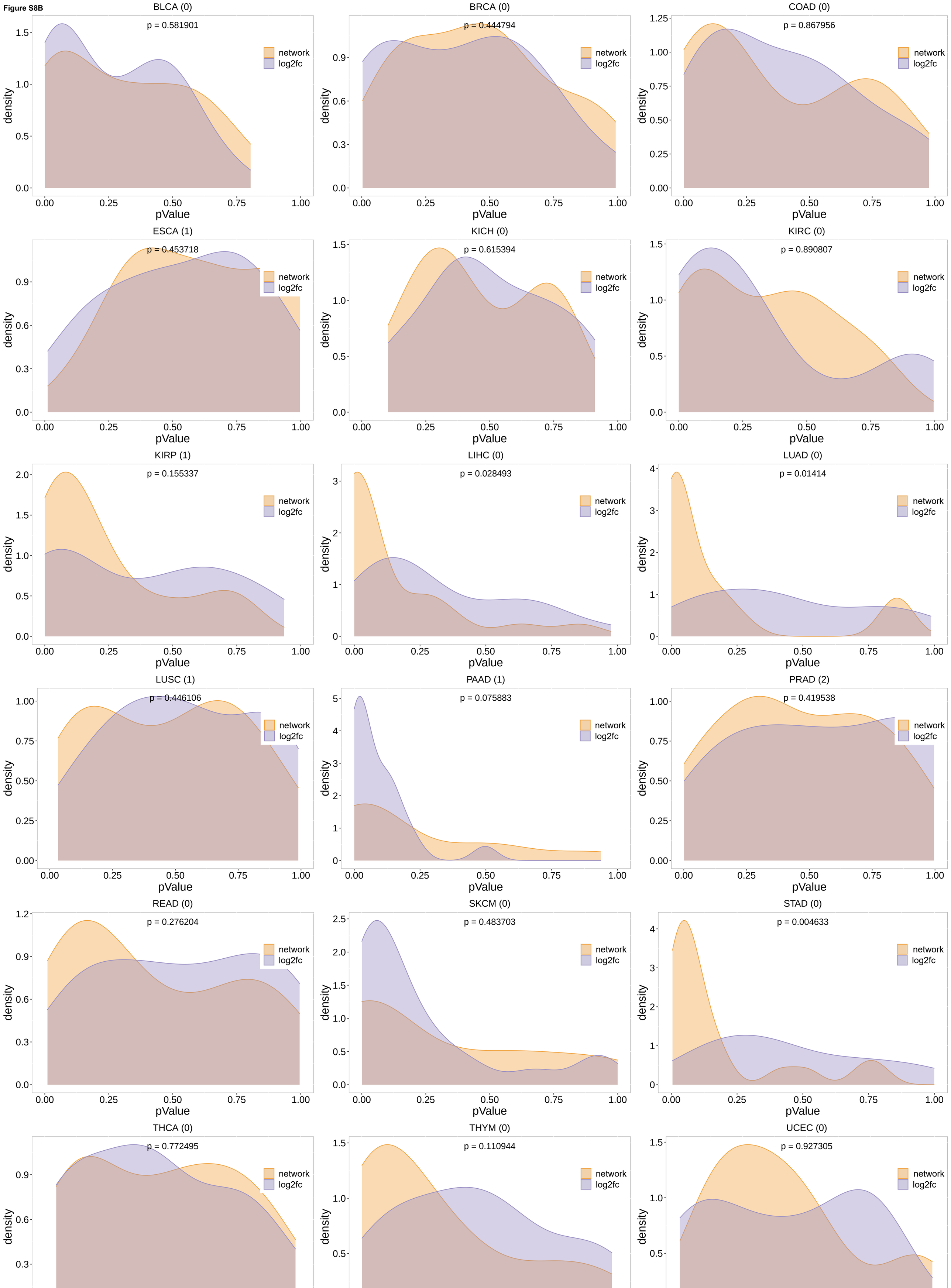
BLCA (0)
p = 0.581901
BRCA (0)
p = 0.444794
COAD (0)
p = 0.867956
ESCA (1)
p = 0.453718
KICH (0)
p = 0.615394
KIRC (0)
p = 0.890807
KIRP (1)
p = 0.155337
LIHC (0)
p = 0.028493
LUAD (0)
p = 0.01414
LUSC (1)
p = 0.446106
PAAD (1)
p = 0.075883
PRAD (2)
p = 0.419538
READ (0)
p = 0.276204
SKCM (0)
p = 0.483703
STAD (0)
p = 0.004633
THCA (0)
p = 0.772495
THYM (0)
p = 0.110944
UCEC (0)
p = 0.927305
network
log2fc
density
pValue

Figure S8C

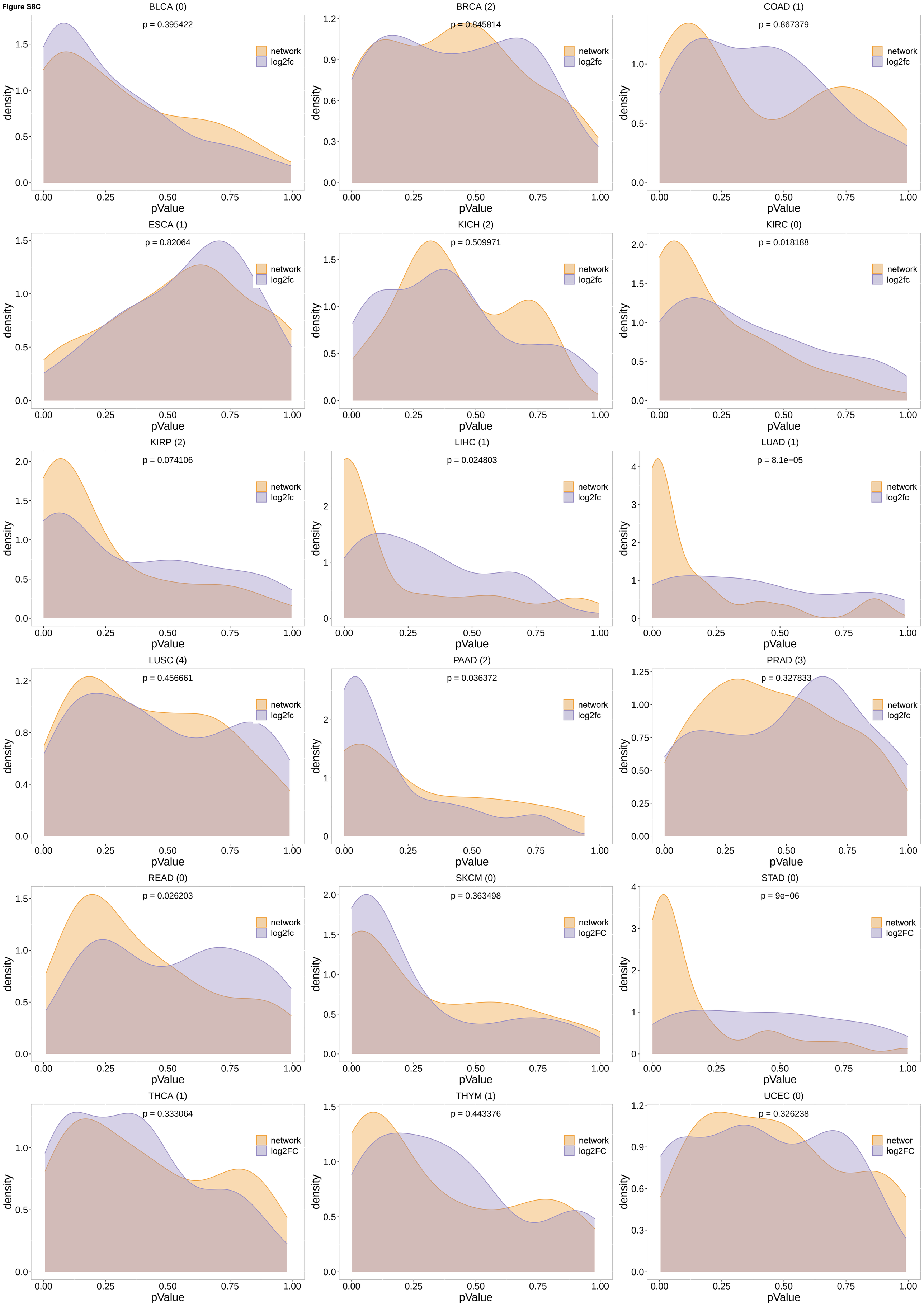
BLCA (0)
p = 0.395422
BRCA (2)
p = 0.845814
COAD (1)
p = 0.867379
ESCA (1)
p = 0.82064
KICH (2)
p = 0.509971
KIRC (0)
p = 0.018188
KIRP (2)
p = 0.074106
LIHC (1)
p = 0.024803
LUAD (1)
p = 8.1e−05
LUSC (4)
p = 0.456661
PAAD (2)
p = 0.036372
PRAD (3)
p = 0.327833
READ (0)
p = 0.026203
SKCM (0)
p = 0.363498
STAD (0)
p = 9e−06
THCA (1)
p = 0.333064
THYM (1)
p = 0.443376
UCEC (0)
p = 0.326238
network
log2fc
log2FC
density
pValue

Figure S8D

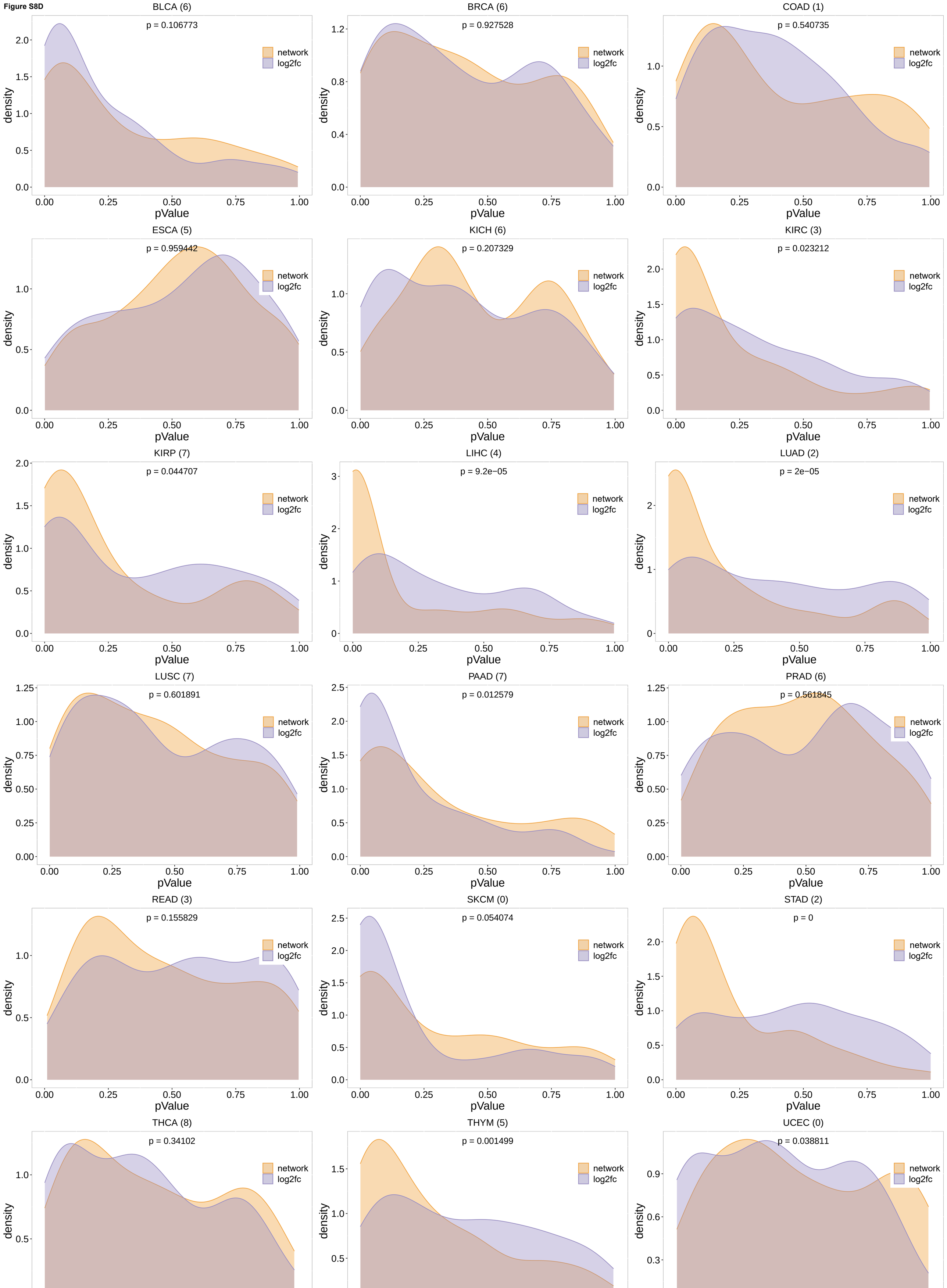
BLCA (6)
p = 0.106773
BRCA (6)
p = 0.927528
COAD (1)
p = 0.540735
ESCA (5)
p = 0.959442
KICH (6)
p = 0.207329
KIRC (3)
p = 0.023212
KIRP (7)
p = 0.044707
LIHC (4)
p = 9.2e−05
LUAD (2)
p = 2e−05
LUSC (7)
p = 0.601891
PAAD (7)
p = 0.012579
PRAD (6)
p = 0.561845
READ (3)
p = 0.155829
SKCM (0)
p = 0.054074
STAD (2)
p = 0
THCA (8)
p = 0.34102
THYM (5)
p = 0.001499
UCEC (0)
p = 0.038811
network
log2fc
density
pValue

Figure S9A

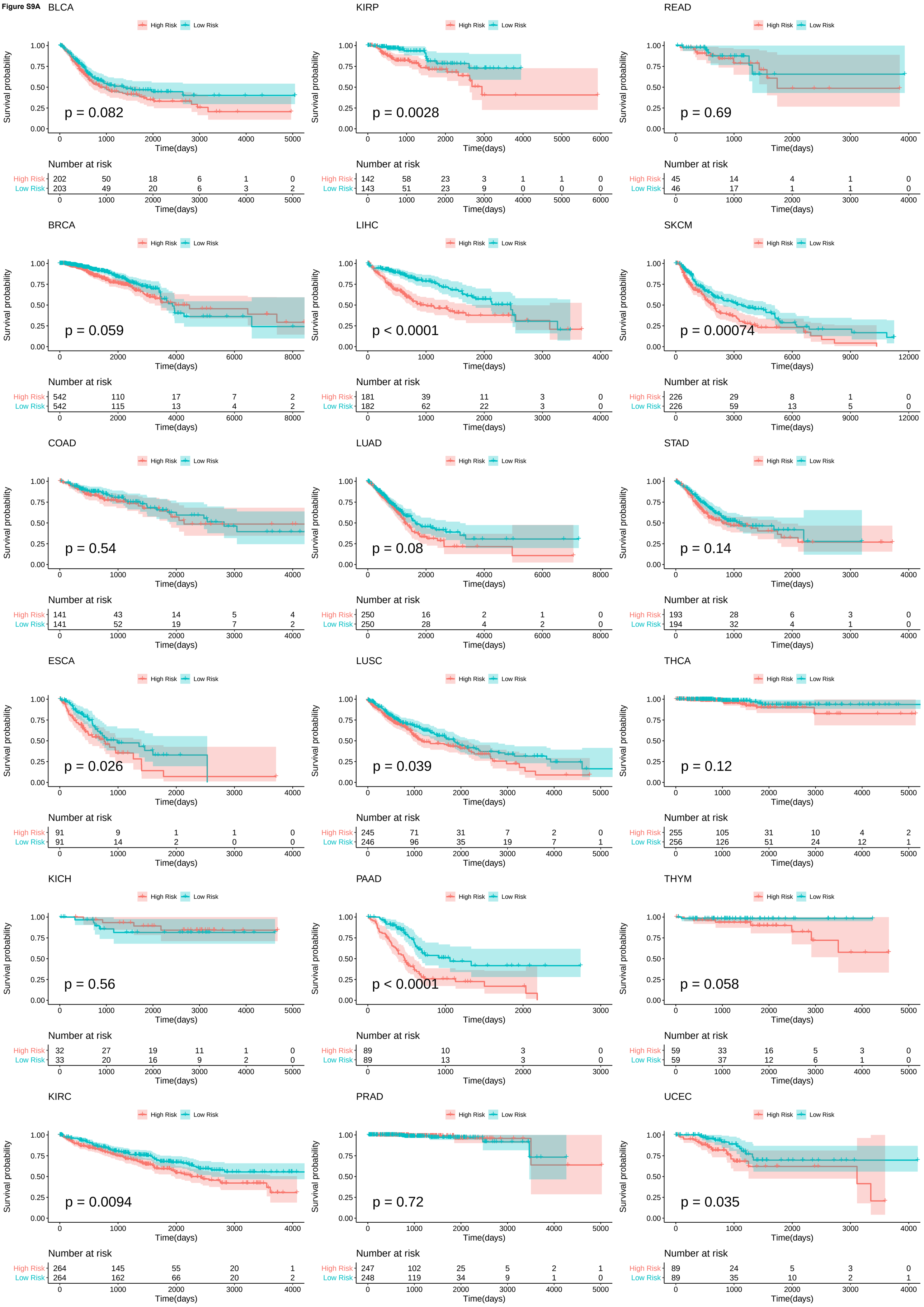
BLCA
High Risk
Low Risk
Survival probability
p = 0.082
Time(days)
Number at risk
High Risk 202 50 18 6 1 0
Low Risk 203 49 20 6 3 2
KIRP
p = 0.0028
High Risk 142 58 23 3 1 1 0
Low Risk 143 51 23 9 0 0 0
READ
p = 0.69
High Risk 45 14 4 1 0
Low Risk 46 17 1 1 0
BRCA
p = 0.059
High Risk 542 110 17 7 2
Low Risk 542 115 13 4 2
LIHC
p < 0.0001
High Risk 181 39 11 3 0
Low Risk 182 62 22 3 0
SKCM
p = 0.00074
High Risk 226 29 8 1 0
Low Risk 226 59 13 5 0
COAD
p = 0.54
High Risk 141 43 14 5 4
Low Risk 141 52 19 7 2
LUAD
p = 0.08
High Risk 250 16 2 1 0
Low Risk 250 28 4 2 0
STAD
p = 0.14
High Risk 193 28 6 3 0
Low Risk 194 32 4 1 0
ESCA
p = 0.026
High Risk 91 9 1 1 0
Low Risk 91 14 2 0 0
LUSC
p = 0.039
High Risk 245 71 31 7 2 0
Low Risk 246 96 35 19 7 1
THCA
p = 0.12
High Risk 255 105 31 10 4 2
Low Risk 256 126 51 24 12 1
KICH
p = 0.56
High Risk 32 27 19 11 1 0
Low Risk 33 20 16 9 2 0
PAAD
p < 0.0001
High Risk 89 10 3 0
Low Risk 89 13 3 0
THYM
p = 0.058
High Risk 59 33 16 5 3 0
Low Risk 59 37 12 6 1 0
KIRC
p = 0.0094
High Risk 264 145 55 20 1
Low Risk 264 162 66 20 2
PRAD
p = 0.72
High Risk 247 102 25 5 2 1
Low Risk 248 119 34 9 1 0
UCEC
p = 0.035
High Risk 89 24 5 3 0
Low Risk 89 35 10 2 1

Figure S9B

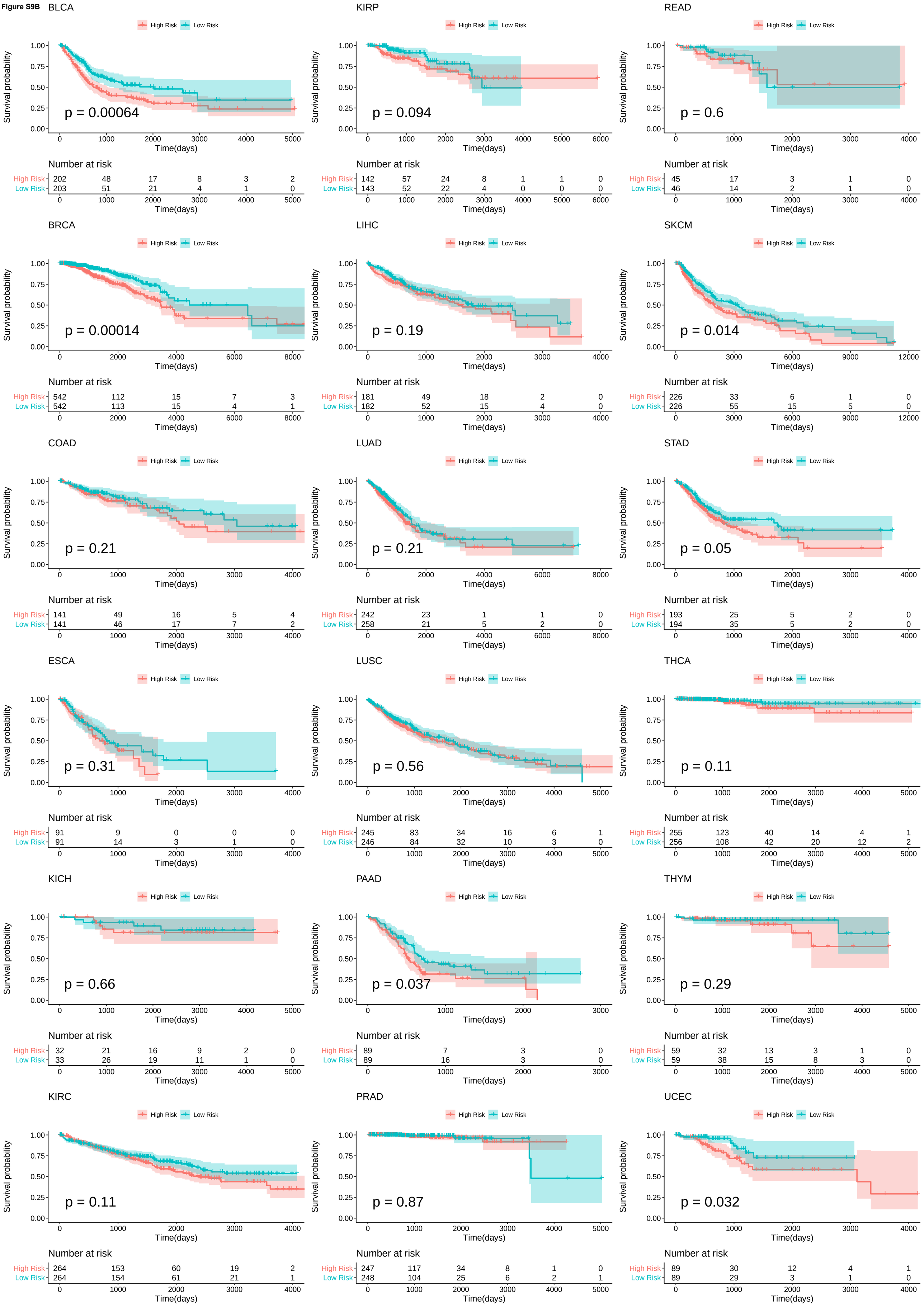
BLCA
High Risk
Low Risk
Survival probability
p = 0.00064
Time(days)
Number at risk
High Risk 202 48 17 8 3 2
Low Risk 203 51 21 4 1 0
KIRP
p = 0.094
Number at risk
High Risk 142 57 24 8 1 1 0
Low Risk 143 52 22 4 0 0 0
READ
p = 0.6
Number at risk
High Risk 45 17 3 1 0
Low Risk 46 14 2 1 0
BRCA
p = 0.00014
Number at risk
High Risk 542 112 15 7 3
Low Risk 542 113 15 4 1
LIHC
p = 0.19
Number at risk
High Risk 181 49 18 2 0
Low Risk 182 52 15 4 0
SKCM
p = 0.014
Number at risk
High Risk 226 33 6 1 0
Low Risk 226 55 15 5 0
COAD
p = 0.21
Number at risk
High Risk 141 49 16 5 4
Low Risk 141 46 17 7 2
LUAD
p = 0.21
Number at risk
High Risk 242 23 1 1 0
Low Risk 258 21 5 2 0
STAD
p = 0.05
Number at risk
High Risk 193 25 5 2 0
Low Risk 194 35 5 2 0
ESCA
p = 0.31
Number at risk
High Risk 91 9 0 0 0
Low Risk 91 14 3 1 0
LUSC
p = 0.56
Number at risk
High Risk 245 83 34 16 6 1
Low Risk 246 84 32 10 3 0
THCA
p = 0.11
Number at risk
High Risk 255 123 40 14 4 1
Low Risk 256 108 42 20 12 2
KICH
p = 0.66
Number at risk
High Risk 32 21 16 9 2 0
Low Risk 33 26 19 11 1 0
PAAD
p = 0.037
Number at risk
High Risk 89 7 3 0
Low Risk 89 16 3 0
THYM
p = 0.29
Number at risk
High Risk 59 32 13 3 1 0
Low Risk 59 38 15 8 3 0
KIRC
p = 0.11
Number at risk
High Risk 264 153 60 19 2
Low Risk 264 154 61 21 1
PRAD
p = 0.87
Number at risk
High Risk 247 117 34 8 1 0
Low Risk 248 104 25 6 2 1
UCEC
p = 0.032
Number at risk
High Risk 89 30 12 4 1
Low Risk 89 29 3 1 0
Time(days)

Figure S10

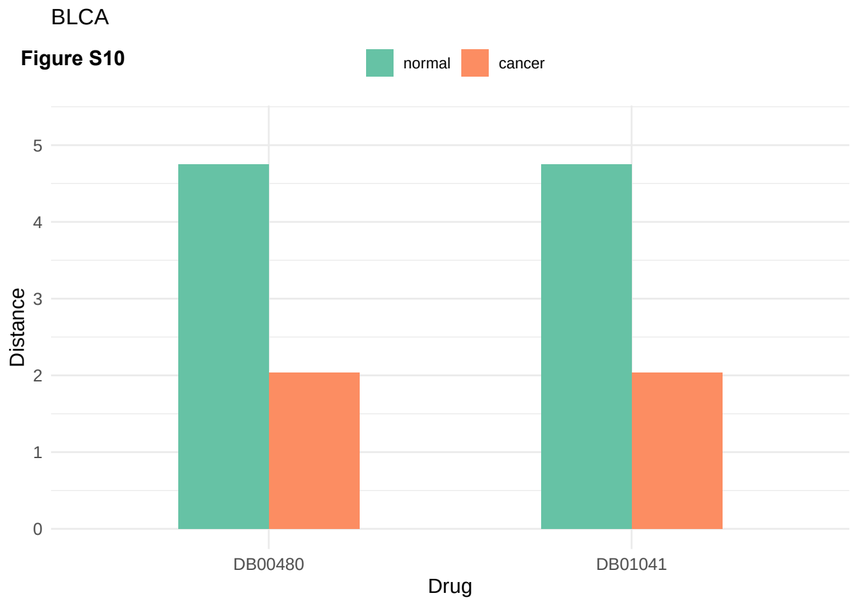
BLCA
normal
cancer
Distance
0
1
2
3
4
5
DB00480
DB01041
Drug

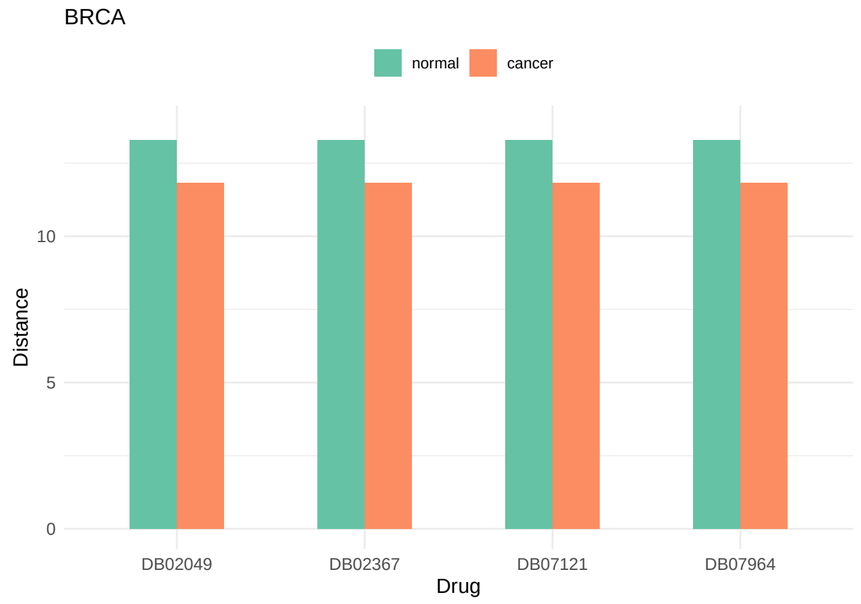
BRCA
normal
cancer
Distance
0
5
10
DB02049
DB02367
DB07121
DB07964
Drug

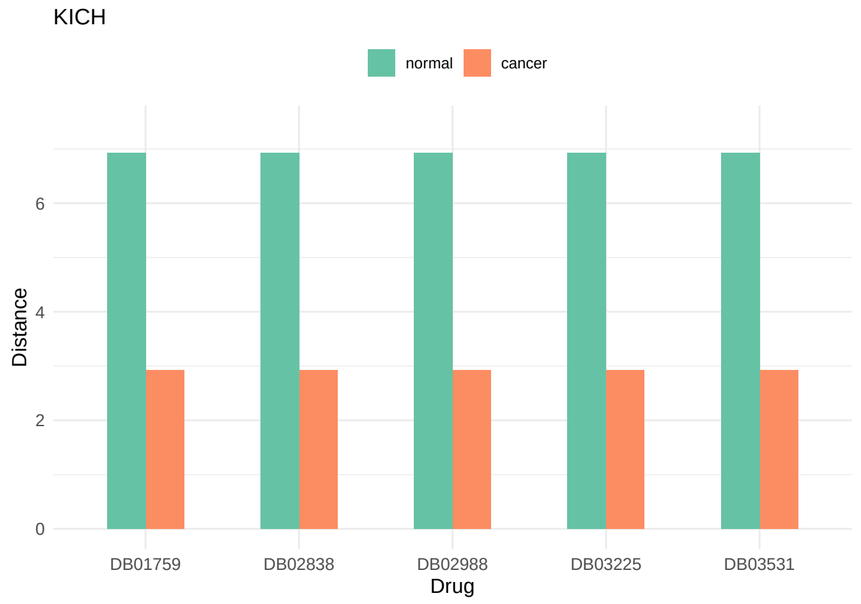
KICH
normal
cancer
Distance
0
2
4
6
DB01759
DB02838
DB02988
DB03225
DB03531
Drug

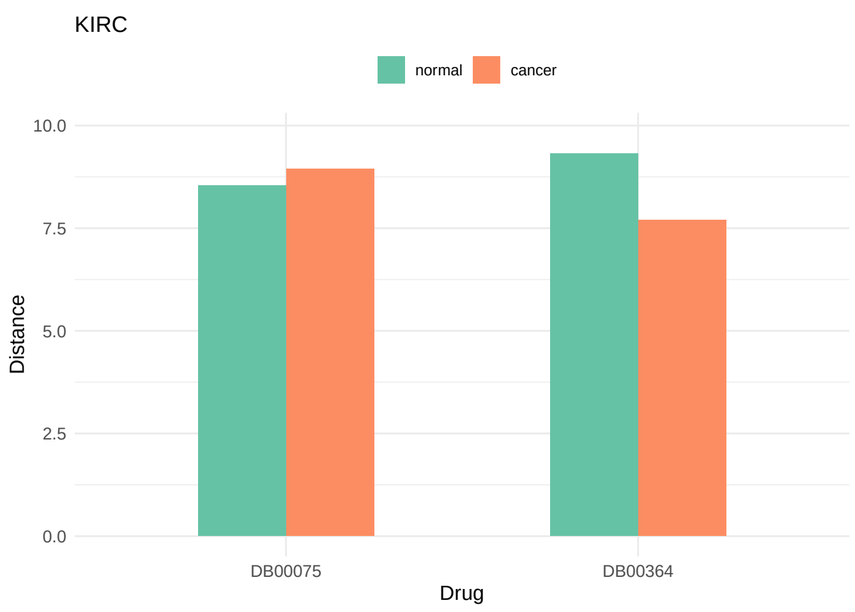
KIRC
normal
cancer
Distance
0.0
2.5
5.0
7.5
10.0
DB00075
DB00364
Drug

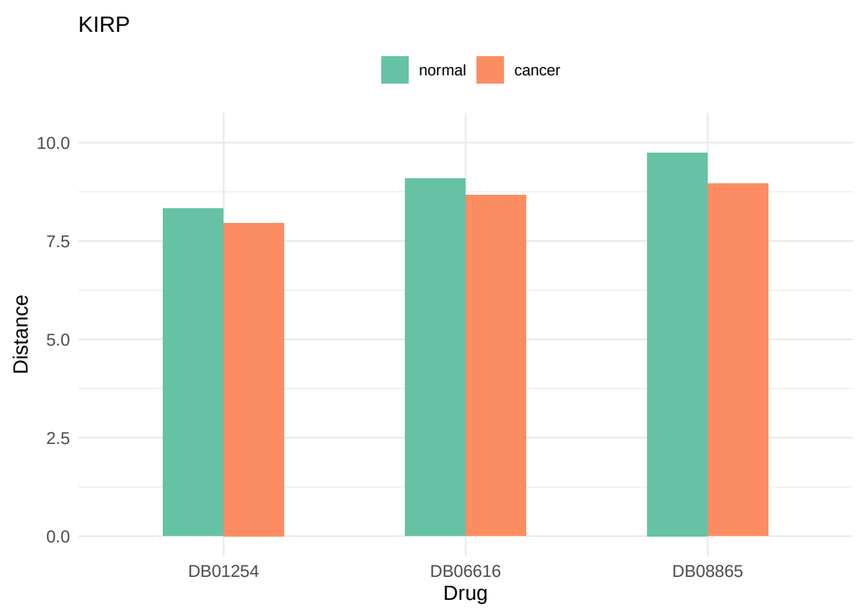
KIRP
normal
cancer
Distance
0.0
2.5
5.0
7.5
10.0
DB01254
DB06616
DB08865
Drug

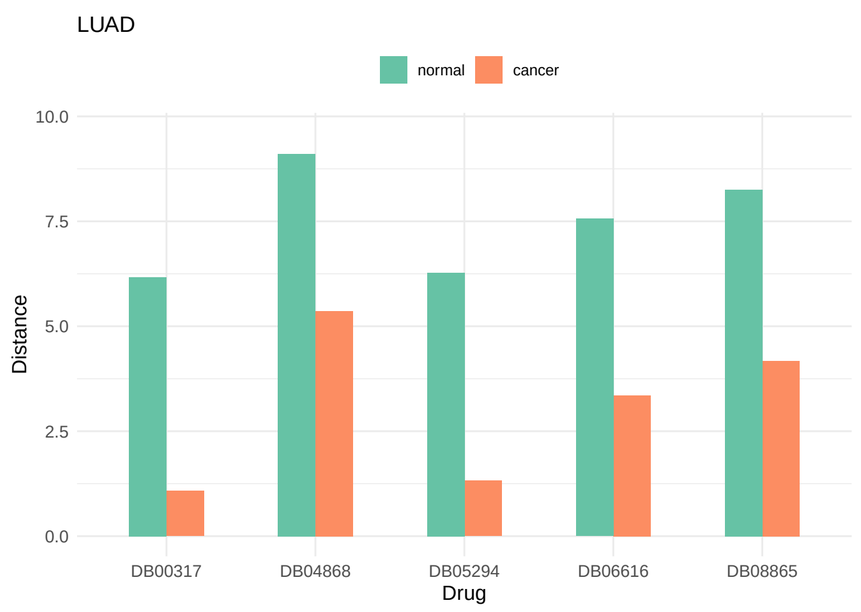
LUAD
normal
cancer
Distance
0.0
2.5
5.0
7.5
10.0
DB00317
DB04868
DB05294
DB06616
DB08865
Drug

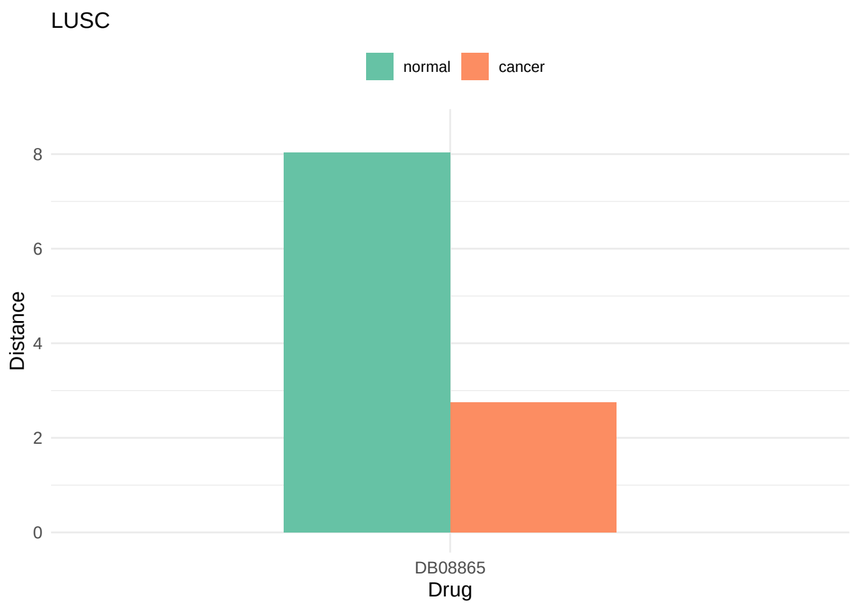
LUSC
normal
cancer
Distance
0
2
4
6
8
DB08865
Drug

Figure S11

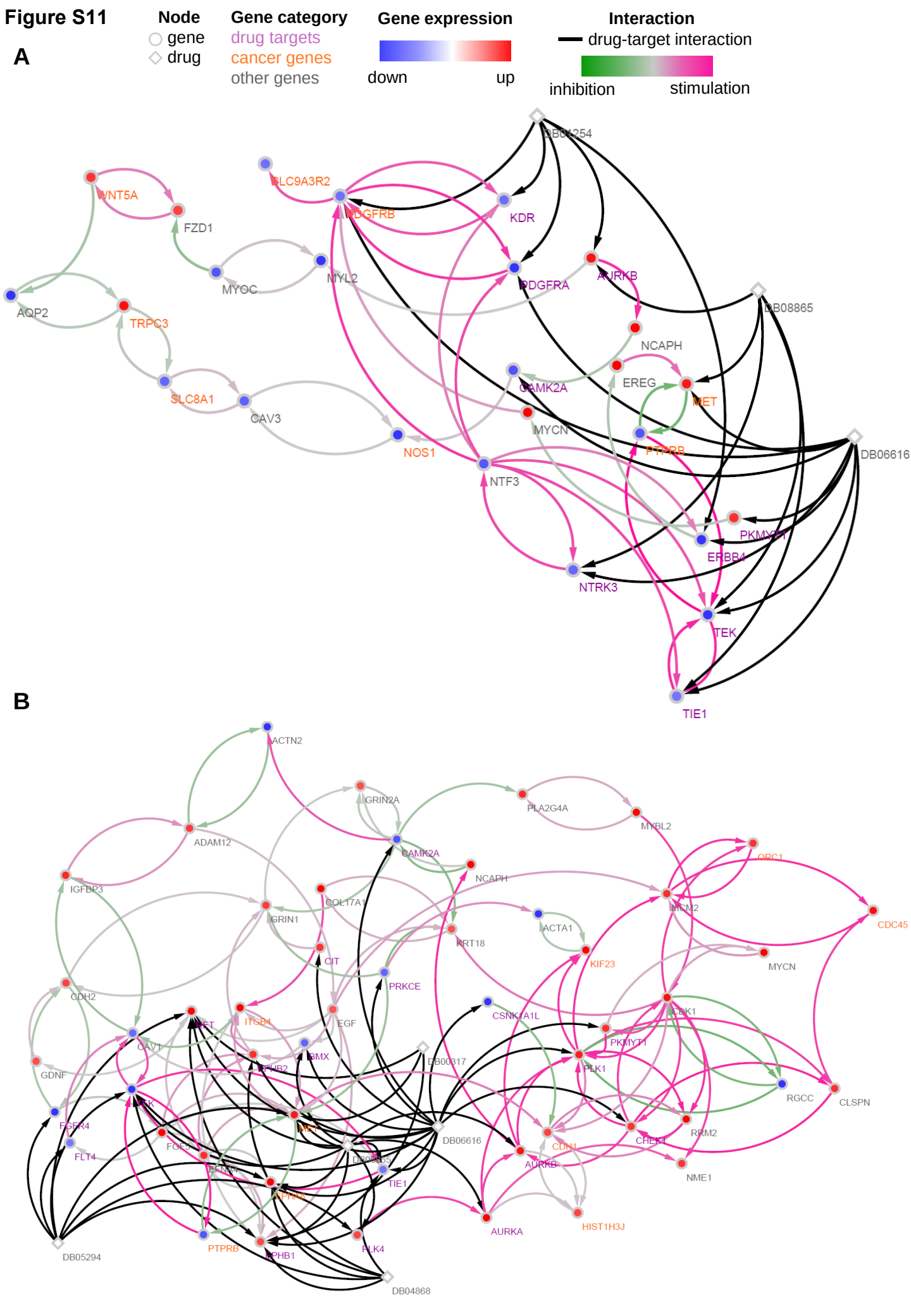
Node
gene
drug
Gene category
drug targets
cancer genes
other genes
Gene expression
down
up
Interaction
drug-target interaction
inhibition
stimulation
A
DB04254
SLC9A3R2
WNT5A
FZD1
PDGFRB
KDR
MYOC
MYL2
PDGFRA
AURKB
DB08865
AQP2
TRPC3
NCAPH
EREG
CAMK2A
MET
SLC8A1
CAV3
MYCN
NOS1
PTPRB
DB06616
NTF3
PKMYT1
ERBB4
NTRK3
TEK
TIE1
B
ACTN2
GRIN2A
PLA2G4A
MYBL2
ADAM12
CAMK2A
ORC1
NCAPH
IGFBP3
COL17A1
MCM2
CDC45
GRIN1
ACTA1
KRT18
KIF23
MYCN
CIT
PRKCE
CDH2
CDK1
ITGB4
EGF
CSNK1A1L
PKMYT1
CAV1
BMX
DB00317
PLK1
GDNF
EPHB2
RGCC
CLSPN
TEK
FGFR4
MET
RRM2
DB06616
FLT4
FGF5
CDH1
CHEK1
AURKB
NME1
TIE1
PTPRB
EPHB1
PLK4
AURKA
HIST1H3J
DB05294
DB04868

Figure S12

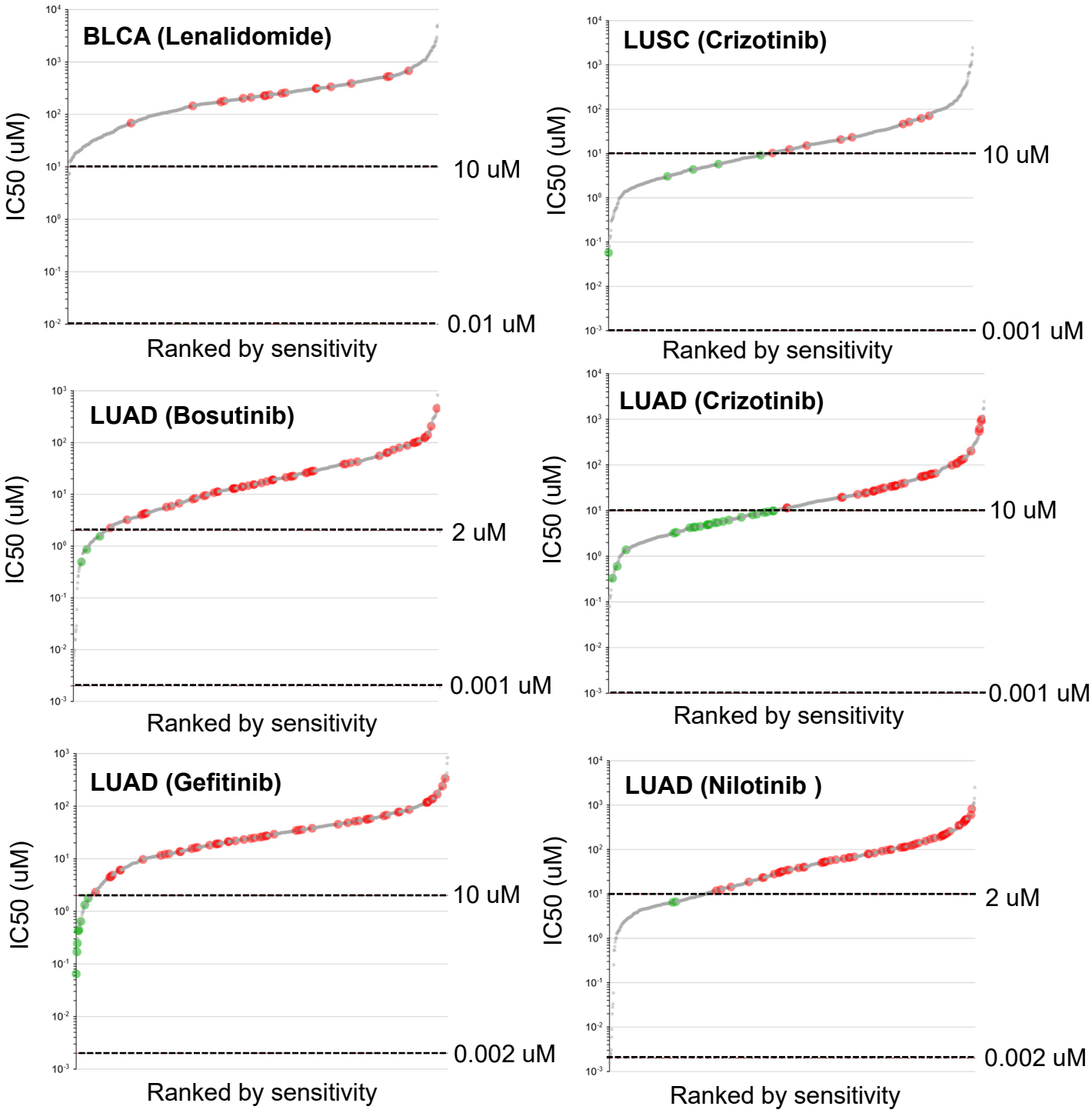
BLCA (Lenalidomide)
IC50 (uM)
10 uM
0.01 uM
Ranked by sensitivity
LUSC (Crizotinib)
IC50 (uM)
10 uM
0.001 uM
Ranked by sensitivity
LUAD (Bosutinib)
IC50 (uM)
2 uM
0.001 uM
Ranked by sensitivity
LUAD (Crizotinib)
IC50 (uM)
10 uM
0.001 uM
Ranked by sensitivity
LUAD (Gefitinib)
IC50 (uM)
10 uM
0.002 uM
Ranked by sensitivity
LUAD (Nilotinib)
IC50 (uM)
2 uM
0.002 uM
Ranked by sensitivity